# JIMMA UNIVERSITY

## JIMMA INSTITUTE OF TECHNOLOGY

## FACULTY OF MECHANICAL ENGINEERING

### MANUFACTURING ENGINEERING STREAM

# Study on Parametric Optimization of Fused Deposition Modeling (FDM) Process

A thesis submitted to the School of Graduate Studies of Jimma University in partial fulfillment of the requirements for award of Degree of Masters of science in Manufacturing System Engineering.


**By**

**Hana Beyene**

**Id. No 0990/09**


**Jimma , Oromia, Ethiopia**

**November, 2018**

# JIMMA UNIVERSITY

## JIMMA INSTITUTE OF TECHNOLOGY

## FACULTY OF MECHANICAL ENGINEERING

### MANUFACTURING ENGINEERING STREAM

# Study on Parametric Optimization of Fused Deposition Modeling (FDM) Process

A thesis submitted to the School of Graduate Studies of Jimma University in partial fulfillment of the requirements for award of Degree of Masters of science in Manufacturing System Engineering.

**By**

**Hana Beyene**

**Id. No 0990/09**

Under the supervision of

**Main advisor: Dr. Barun Haldar (Assis. Prof.)**

**Co advisor: Dr. Timothy (Assis. Prof.)**

**Jimma, Oromi, Ethiopia**

**November, 2018**

# DECLARATION

I, the under signed, declare that this thesis entitled by "Study on Parametric Optimization of Fused Deposition Modeling (FDM) Process" is my original work, and has not been presented by any other person for an award of a degree in this or any other University, and all sources of materials used for the thesis have been properly acknowledged.

**Name: Hana Beyene** (Candidate) ____________________ ____________________

ID No.: RM 0990/09 Signature Date

**Dr. Barun Haldar** ____________________ ____________________

Advisor: Signature Date:

**Dr. Timothy Kwa** ____________________ ____________________

Co-Advisor: Signature Date

**Approved by Board of Examiners**

External Examiner ____________________________ signature _______ Date_______

Internal Examiner ____________________________ signature _______ Date _______

Chair Man ____________________________ signature _______ Date _______

# STATEMENT OF THE AUTHOR

First, I declare that this thesis is my confide work and that all sources of materials used for this thesis have been duly acknowledged. This thesis has been submitted in partial fulfillment of the requirements of M.Sc. degree at Jimma Institute of Technology and is deposited at the University Library to be made available to borrowers under rules of the Library. I solemnly declare that this thesis is not submitted to any other institution anywhere for the award of any academic degree, diploma, or certificate.

Brief quotations from this thesis are allowable without special permission provided that accurate acknowledgement of source is made. Requests for permission for extended quotation from or reproduction of this manuscript in whole or in part may be granted by the head of the major department or the Dean of the School of Graduate Studies when in his or her judgment the proposed use of the material is in the interests of scholarship. In all other instances, however, permission must be obtained from the author.

Name: Hana Beyene Signature: …………………

Place: Jimma Institute of Technology, Jimma, Oromia, Ethiopia

Date of Submission: …………………

# ACKNOWLEDGEMENTS

This thesis is a result of research that has been carried out at Jimma Instutiute of Technology, Jimma**.** During this period, I came across with a great number of people whose contributions in various ways helped my field of research and they deserve special thanks. It is a pleasure to convey my gratitude to all of them. In the first place, I would like to express my deepest gratitude and indebtedness to my supervisors Dr. Barun Haldar and Dr. Timothy for their advice, and guidance from early stage of this research. I specially acknowledge Dr Barun for his advice, supervision, and crucial contribution, as and when required during this research. Dr Timothy, for their kind cooperation, support and concern regarding my sub -Lab requirements in Biomedical lab of this work.

I would like to thank Mr. Abiyu ,testing Lab technician of Mechanical Engineering Department, Addis Ababa Institute of Technology, and Mr. Mitiku, testing lab technician of Mechanical engineering Department, Jimma institute of technology for their whole hearted support and cooperation during the course of this research.

I would like to thank my ever dearest life partner, Amanuel Diriba, who worked hard to help me and being always by my side. I could not have done this study without him, and I will appreciate all his efforts put into my entire academic career for eternity.

Last, but not the least, I thank the one above all of us, the almighty God, for giving me the strength during the period of this research work.

# ABSTRACT

Fused deposition modeling (FDM) is a unique rapid prototyping (RP) technique that uses plastic material in a semi-molten state to fabricate the products directly from a CAD model. FDM is an additive manufacturing method, and prototypes are made layer-by-layer through the addition of semi-molten plastic material onto a platform from bottom to top. Sectors including the medical implant industry need increasingly higher levels of dimensional accuracy, minimal surface roughness and specifically tailored mechanical properties. But traditional FDM methods do not effectively address these needs. Compared with some other conventional method the quality of the FDM fabricated part extensively depends on process variable parameters.

The aim of this research work is to study the effect of process parameters such as layer height, infill, build speed, and build temperature on dimensional accuracy, surface finish, and mechanical properties (e.g. tensile strength) of FDM printed parts. Experiments were conducted using Taguchi's design of experiments consisting of three levels of optimization for four factors. The Taguchi method was used to optimize effect input process parameters on dimensional accuracy, surface finish, and tensile strength. A series of experiments were conducted on parts produced using Flash forge 3D printer from ABS. To analyze the effect of each process parameters on part quality, Taguchi analysis, ANOVA, main effect plots, interaction plots, 3D Surface plots, and Contour plots were used. From the result obtained, response values show that the optimal setting of process parameters for dimensional accuracy (ΔW, ΔT and ΔL) are the layer height at 0.29 mm, infill at 15 %, build speed at 30 mm/min and build temperature at 220 ºC, which yield minimum ΔW 0.0048 at maximum value of S/N ratio 46.3752, ΔT 0.0044 at maximum value of S/N ratio 47.1309 and ΔL 0.0056 at maximum value of S/N ratio = 45.0362. Based on the S/N analysis, the optimal process parameters for surface roughness (Ra) are the same as the ones used for dimensional accuracy, yielding which give a minimum Ra = 7.779 μm at maximum value of S/N ratio - 17.8185. Results of Taguchi optimization indicates that the optimal FDM parameters for Tensile strength (UTS) are the layer height at 0.19mm, the Infill rate at 45 %, Build speed at 180 mm/min and the build temperature at 240 ºC which gives maximum UTS =39.094 MPa at maximum value of S/N ratio = 31.8422.



***KEYWORDS:*** *Fuse deposition modeling, process parameters, Taguchi method, ANOVA*

# Table of Contents

## List of Tables

**No table of figures entries found.**

## List of Figures

## Nomenclature

| | |
|---|---|
| FDM | Fuse deposition modeling |
| RP | Rapid prototyping |
| CAD | Computer aided design |
| 3D | Three dimensions |
| ABS | Acrylonitrile Butadiene Styrene |
| DOE | Design of experiment |
| ANOVA | Analysis of variance |

| | |
|---|---|
| STL | Stereo lithography |
| SLS | Selective laser sintering |
| LOM | Laminated object manufacturing |
| $\Delta W$ | Change in width |
| $\Delta T$ | Change in thickness |
| $\Delta L$ | Change in length |
| Ra | Surface roughness |
| UTS | Ultimate Tensile strength |

# Chapter 1

# Introduction

## 1.1 Introduction

In any manufacturing process Customers do not like to wait for products. Fast changing customer demand and increased competitiveness in marketplace forced the industries to rethink the way products are designed resulting in introduction of new technologies for part fabrication. There for, in this case processing time needs to be shortened by avoiding nonproductive times needed to be eliminated. The traditional method involves time loss on concept designing, manufacturing, assembly and testing. For instance, in foundry technology, lot of time is spent until a satisfactory product is developed. This core factor and other drawbacks of traditional method lead to modify the way the products are being designed and produced. The endeavor on reduction of product development time has resulted in the birth of a new generation of production equipment which manufacture part directly from the its CAD (computer aided design) model on a layer by layer deposition principle without tools, dies, fixtures and human intervention[1].This technology is known as Rapid prototyping.

The rapid prototyping (RP) technology is a cheap, flexible and fast way to the fabrication of parts from CAD model. FDM is one of the RP technique that is used for fabricating solid prototypes in various materials directly from a computer-aided design (CAD) data[2][3]. In this study, an Acrylonitrile-Butadiene-Styrene (ABS) thermoplastic polymer is extruded through a heated nozzle to deposit the layers. The controlled extrusion head deposits very thin beads of material in semi molten state onto the build platform to form the first level. After the platform lowers, the extrusion head places a second layer upon the first. Supports are fabricated along the path; tie up to the part either with a second weaker material or with a perforated junction [4][5].

When setting the printing options of the machine, several process parameters have to be taken into account, such as temperature, speed, infill densities etc., that directly influence the quality (such as dimensional accuracy, surface roughness, tensile strength) of the fabricated parts. Selecting these parameters also a great challenge for the users and is generally solved by experience without considering their influence on the product. The surface finish of parts obtained through these manufacturing processes is important, especially in cases where the components are in contact with other elements or materials in their service life. For example, building molds to produce components by means of Solid Free Form Manufacturing Processes. Dimensional accuracy is extremely important in any product-development cycle as it directly affects part functionality. inaccuracy of the parts being built by RP technology is one of the major challenges that needs to be overcome[6][7].

## 1.2 Overview of rapid prototyping process

Rapid prototyping is a technology for quickly fabricating physical models, functional prototypes and small batches of parts directly from computer-aided design (CAD) data[9]. In RP system a CAD model is further changed into a thin slices/layered model and according to these slicing data, the material is deposited in a form of layers. Process, solid freedom fabrication and layer based fabrication. In RP system three types of materials, namely solid form, liquid form or powder form are used for fabrication of different parts. CAD software play a virtual role in RP system. With CAD software we can design a complex shape part easily[10]. The first methods for rapid prototyping became available in the late 1980s and were used to produce models and prototype parts. Today, they are used for a wide range of applications and are used to manufacture production-quality parts in relatively small numbers if desired without the typical unfavorable short-run economics[11]. What is commonly considered to be the first RP technique, Stereo lithography, was developed by 3D Systems of Valencia, CA, USA. The company was founded in 1986, and since then, a number of different RP techniques have become available[12].

The main advantage of the system is that almost any shape can be produced. Time and money savings vary from 50 – 90 % compared to conventional systems[13]. No tooling is required to manufacture parts of complex geometry just by tracing the CAD model layer by layer. The ability to manufacture complex parts helps us to substantially reduce production cost, a concept not possible in traditional manufacturing where complexity in design directly resulted in increased cost due to increased cost of machining. One of the other advantages of RP technologies is their ability to produce functional assemblies by consolidating sub-assemblies into one unit thereby reducing the part count, handling time storage requirement. In addition, error can be detected at an early stage. In spite of such added advantages it is not possible to implement on a full scale at industrial level because of its limitations in terms of type of product manufactured. Resolution is not as fine as traditional machining (millimeter to sub-millimeter resolution) Surface flatness is rough[14] [15].

### 1.2.1 Basic process of RP

All rapid prototyping techniques consist of the following basic stages:

1. Development of CAD model.
2. Conversion of CAD model into STL format.
3. Slice the STL model into a number of thin layers.
4. Construct the model one above the other so that layers are approximation of model.
5. Clean and finish the model.

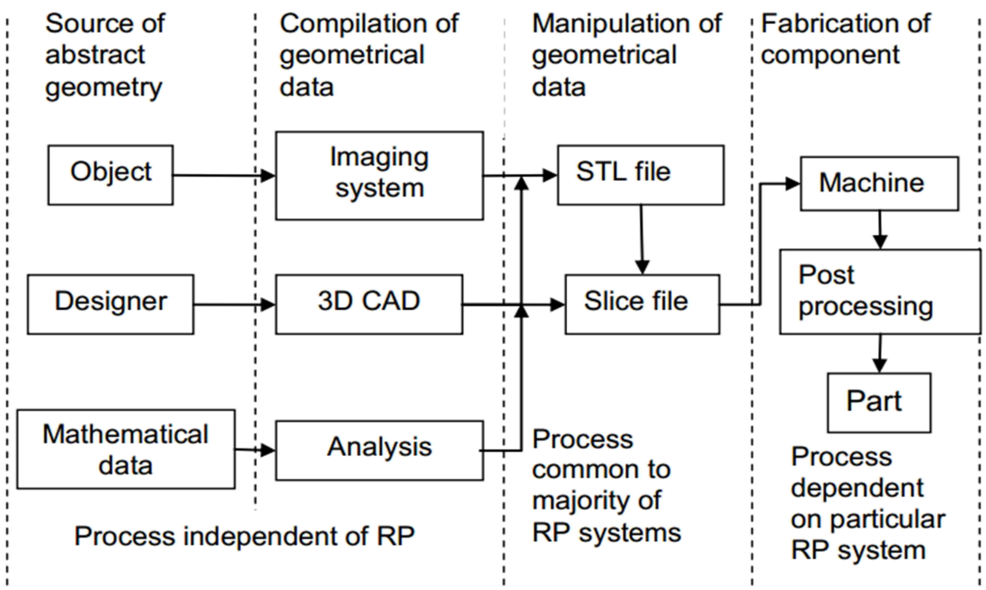


Figure 1.1 Main process stages common to most rapid prototyping systems[16].

**1. Development of a CAD model**: The process begins with the generation of CAD model of the desired object which can be done by converting the existing two dimensional drawing or by creating a new part in CAD in various solid modeling packages.

**2. Conversion to STL Format;** Since different CAD software use different algorithms for creation of 3D model STL format is used as a standard by all the prototyping applications. It consists of a number of triangle shaped planar structure which when together stacked on one another are used to approximate the model. This format also stores all information about the coordinates and normal vectors of all the planar surfaces.

**3. Slice the STL File**: In the third step, a pre-processing program prepares the STL file to be built. Several programs are available, and most allow the user to adjust the size, location and orientation of the model. Build orientation is important for several reasons. First, properties of rapid prototypes vary from one coordinate direction to another. For example, prototypes are usually weaker and less accurate in the z (vertical) direction than in the x-y plane. In addition, part orientation partially determines the amount of time required to build the model. Placing the shortest dimension in the z direction reduces the number of layers, thereby shortening build time. The pre-processing software slices the STL model into a number of layers from 0.01 mm to 0.7 mm thick, depending on the build technique. The program may also generate an auxiliary structure to support the model during the build. Supports are useful for delicate features such as overhangs, internal cavities, and thin-walled sections. Each PR machine manufacturer supplies their own proprietary pre-processing software.

**4. Layer by Layer Construction**: The fourth step is the actual construction of the part. Using one of several techniques (described in the next section) RP machines build one layer at a time from polymers, paper, or powdered metal. Most machines are fairly autonomous, needing little human intervention.

**5. Clean and Finish**: The final step is post-processing. This involves removing the prototype from the machine and detaching any supports. Some photosensitive materials need to be fully cured before use. Prototypes may also require minor cleaning and surface treatment. Sanding, sealing, and/or painting the model will improve its appearance and durability.

### 1.2.2 Types of RP techniques

**1. Stereo lithography (SLA)**

This is based on selective polymerization of a photosensitive resin using ultraviolet light. In this system, an ultraviolet laser beam is focused on the top layer of photo sensitive resin contained in a vat. The beam is positions and moved in horizontal X and Y directions to polymerize the resin within the boundary a particular cross-section. The cured layer of polymer is lowered by a platform attached to it, so that a fresh layer of liquid resin covers the cured layer[17]. Even though there are still many limitations to this process such as: Requires post-curing, Support structures always needed, to Remove support structures can be difficult, Limited materials (Photo polymers), Some war page, shrinkage and curl due to phase change. This technique have main advantages like to  achieving accuracy in industries, Market shares and industry presence, Capable of high detail and thin walls, Good surface finish[19].

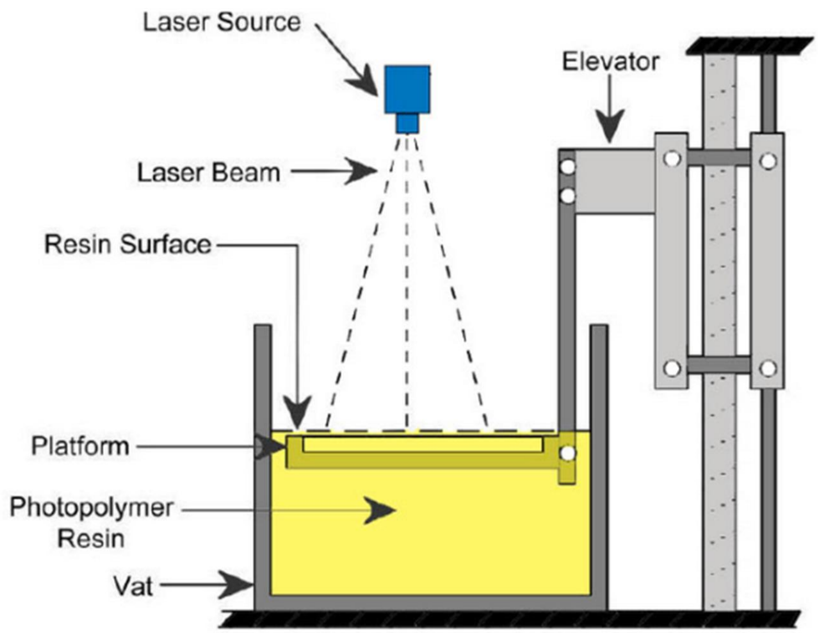


Figure 1.2 Schematic of stereo lithography [18]

**2. Selective laser sintering (SLS)**

In this process a high power carbon dioxide laser beam selectively melts and fuses powdered material spread on a layer[20]. The powder is metered in precise amounts and is spread by a counter-rotating roller on the table. A laser beam is used to fuse the powder within the section boundary through a cross-hatching motion. The table is lowered through a distance corresponding to the layer thickness (usually 0.01 mm) before the roller spreads the next layer of powder on the previously built layer. The un sintered powder serves as the support for overhanging portions, if any in the subsequent layers[21]. The main advantage is that the fabricated prototypes are porous (typically 60% of the density of molded parts), thus impairing their strength and surface finish, Variety of materials, no post curing required, Fast build times, Limited use of support structures.  However, Rough surface finish, Mechanical properties below those achieved in injection molding process for same material. Many build variables, complex operation, Material changeover difficult compared to FDM & SLA, some post-processing / finishing required are the main limitation of this process[23].

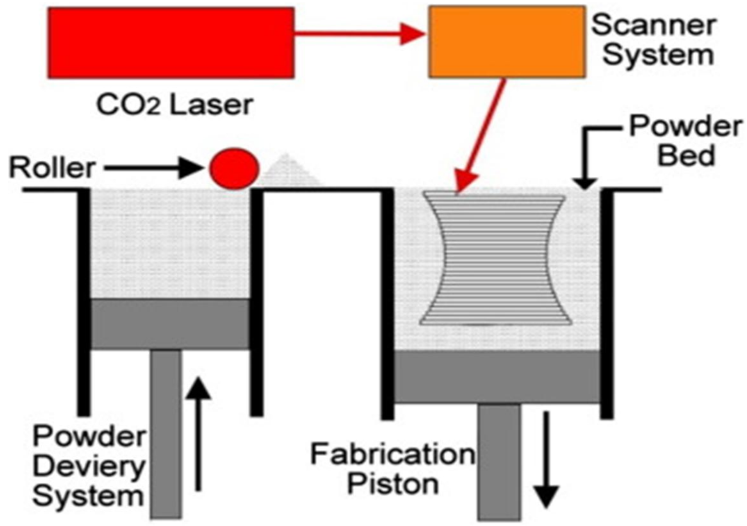


Figure 1.3 Schematic of selective laser sintering[22]

**3. Laminated object manufacturing**

Laminated object manufacturing included layer-by-layer overlay of paper material sheet, cut utilizing a laser, every sheet speaking to one cross-sectional layer of the CAD model of the part. In laminated object manufacturing the segment of the paper sheet which is not contained inside the last part is cut into 3D shapes of materials utilizing a cross-lid cutting operation. This procedure has been created taking into account sheet cover including other form materials and cutting procedures. In view of the development guideline, just the external shape of the parts is cut and the sheet can be either cut and after that stacked or stacked and afterward cut[24].The main advantage is that its ability to produce larger-scaled models, Uses very inexpensive paper, Fast and accurate, Good handling strength, environmentally friendly, Not health threatening. However, this technique has its own disadvantages such as Need for decubing, which requires a lot of labor, can be a fire hazard finish, accuracy and stability of paper objects not as good as materials used with other RP methods[26].

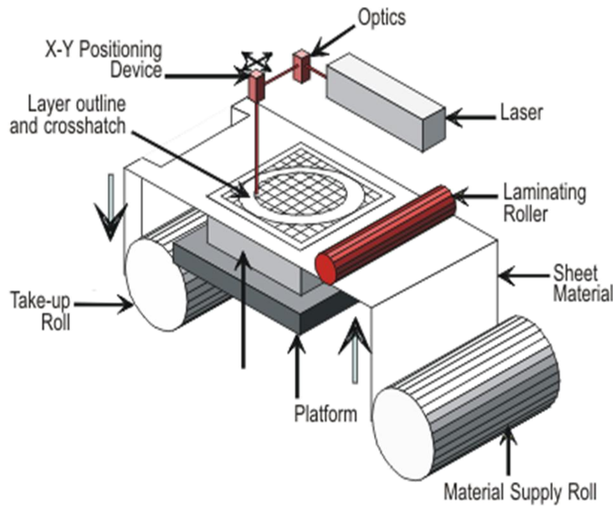


Figure 1.4 Schematic of an LOM setup[25]

**4. Fused deposition modeling**

FDM was developed by S. Scott Crump in the late 1980s and was commercialized in 1990 by Stratasys. FDM begins with the same STL-format file downloaded to the machine, as does any other 3D technology. The program is slicing the model, orienting and preparing it for the building process. If it is necessary, support structures are generated. FDM works by laying down molten plastic fiber, layer-by-layer from a heated nozzle onto a platform according to the 3D model. The nozzle can be moved in different directions (horizontal and vertical) by a numerically controlled mechanism. Once it is deposited in the proper direction, the material rapidly cools down and hardens, bonding with the previous layer[27] .

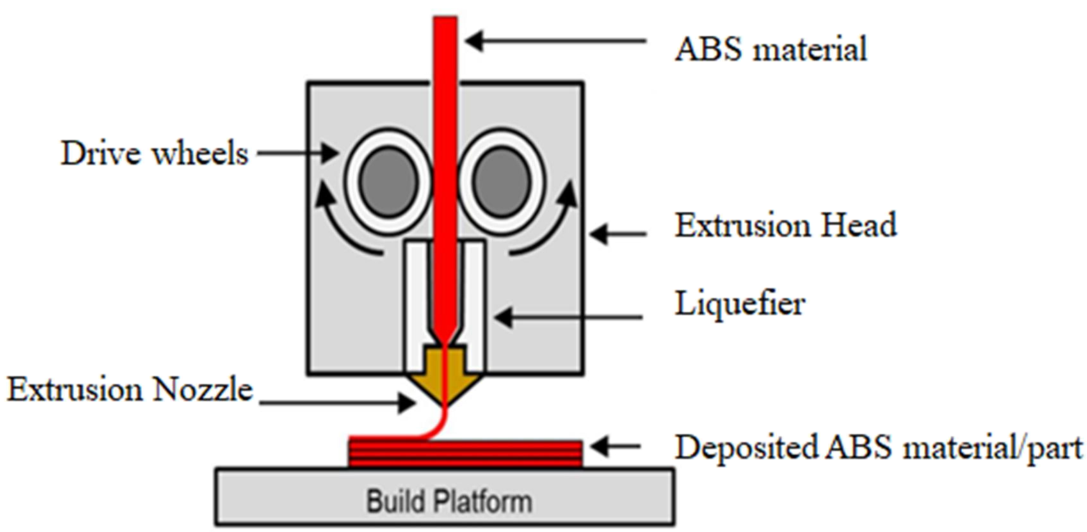

Figure 1.5 schematic of FDM[28]

## 1.3 Objectives of the research

### 1.3.1 General objective

The main objective of the present work is studies focused on experimental investigations to analysis and optimize impact of Flash Forge Fuse deposition modeling (FDM) process parameters on quality of part produced.

### 1.3.2 Specific objectives

- to reduce the relative change in, width (ΔW) length (ΔL), and thickness (ΔT) respectively.
- To reduce the surface roughness of 3D printed parts.
- To increase the Tensile strength of 3D printed parts.
- Improving quality of part produced using flash forge FDM by controlling and optimizing the process parameters.

## 1.4 Scope of research

This research work mainly focused on one of the Rapid prototyping that is Fused deposition modeling. In order to achieve the objective notified earlier, the following scopes have been recognized:

- The machine used is Flash forge 3D printer.
- Process parameters have been determined before doing the experiment and the quality of the part printed on the printer determined by measuring dimensional accuracy, surface roughness and tensile strength of the product.
- Four process parameters such as layer height, infill, build speed and build temperature have been used.
- Quality of each part measured in terms of Dimensional accuracy (DA), Surface roughness (Ra) and Tensile strength (UTS).
- The result of experimental data will be analyzed using Taguchi analysis, main effect plots, Interaction plots, 3D Surface plots and Contour plots.
- Taguchi method will be used to optimize process parameters in terms of response.
- Material used is ABS

## 1.5 Problem statement

Nowadays focuses has shifted from traditional product development methodology to rapid fabrication techniques because reduction of product development cycle time is a major issue in industries to remain competitive in market. RP is an efficient technology. Due to its ability to build functional parts having complex geometrical shapes within a few minutes FDM is Rapid prototyping technology.

It is mention that different process parameters have effects on the part quality of FDM. Essentially the quality characteristics of FDM build part such as dimensional accuracy, tensile strength; yield strength, dimensional accuracy, production time and surface roughness are the primary concerns to manufactures and users. Deciding on the optimal process parameters to improve surface finish, mechanical properties, material consumptions and build time is still a challenging job for everyone. However, there are still no perfect optimal condition for all for all types of parts produced by FDM. Most parts need better parameters to fulfill these disabilities. The qualities of printed parts using FDM highly depend on selected process parameters. Therefore, it is important to investigate and optimize effect of input process parameters on part produced or outcome response. In traditional part fabrication on FDM, the dimensional accuracy is large, surface roughness is not uniform and tensile strength is not improved due to this, quality of the fabricated part may get affected. To get minimum change in dimension and surface finish and great tensile strength the input parameter of Flash forge creator pro FDM should be optimized. Thus to improve the quality of FDM fabricated parts additional research should be carried out.

## 1.6 Motivation

Currently Rapid prototyping Techniques are used more and more in many industrial branches, such as aerospace, automotive, defense and biomedical, to manufacture functional parts and end-use products rather than prototypes. Therefore, the parts are required to possess sufficient mechanical properties and quality to meet the requirements needed of their applications. In order to bridge this gap, research efforts have been made to develop of the mechanical properties of components as well as their surface quality and geometric accuracy.

## 1.7 Study environment

The study was done on the premises of Jimma University and Addis Ababa University. The experimental setup was done in two mechanical labs, namely surface topography measurement laboratory and material strength testing laboratory and one biomedical lab where three-dimensional printing of the designed samples was conducted. The various reading for the experimental setups was performed in the measurement lab. The experimental setup and measurement were done with the help and guidance of laboratory supervisors.

# Chapter 2
## LITERATURE REVIEW

In last era, many researches were done in the rapid prototyping and tooling techniques in a specific product development. These were having been in the view of methods, products and development of products in various applications. There also various related studies that prove dimensional accuracy of RP systems is still a significant obstacle that is preventing RP technology moving towards becoming a primary production process. Mechanical properties are essential key characteristics of RP systems when considering RP to produce tooling or functional parts. Selecting these parameters is often a great challenge for the user, and is generally solved by experience without considering the influence of variations in the parameters on the mechanical properties of the printed parts[7]. when RP was introduced in the beginning, the materials that were used in these processes to produce components had low yield strength. However, through advancements in material science, the photopolymers and thermoplastics used now have much higher yield strengths[29].

Therefore, any attempt to develop functionally reliable part from FDM process should also necessarily involve the fundamental studies of various process parameters. Earlier studies have reported that FDM parameters such as layer thickness, air gap, raster width, and raster orientation were significantly impacting the quality characteristics of build parts[30][31][32][33].

In relevant empirical studies, parametric optimization was used to develop the quality characteristics of FDM parts or the process performance where the number of FDM process parameters were studied and optimized. Tusharkumar B et al.[34] and J. Cantrell et al.[35]investigated the elasticity performance of ABS material. Similarly, N.Saleh et al. [36], K.Raney et al.[37], and B. Patel et al. [38]investigated the tensile strength of FDM parts. G. Arumaikkannu et al. [39] and X. Zhang et al.[40] optimized the FDM process parameters improving the surface roughness of build parts, while S. Adamczak et al. [41], M. Ibrahim et al., Azila et al. [42] and N.Sudin1 et al. [43]have looked into the dimensional accuracy of FDM parts. These previous studies investigated a single outcome quality response while some studies were done in parametric optimization by investigating multiple quality objectives responses such as Sukindar et al.[44], A.Kohad et al[45] and F.Ali et al.[46] They suggested that building a functional part is attributed to various loading environments in practice. Consequently, process parameters require to be studied in such a way that they are collectively optimized simultaneously, rather than optimize a single quality response.

## 2.1 Applications of rapid prototyping

The first RP system in 1988, has been implemented successfully in the industries of, aerospace, electronics, automotive, toy and so on[47]. In divergence to traditional machining methods, the majority of RP systems tend to manufacture parts based on additive manufacturing process, rather than detraction or removal of material. Therefore, this type of fabrication is unrestricted by the limitations attributed to conventional machining approaches[48].

The time and cost consideration favors prototype production using RP because more time is available for design iteration and optimization [49],[50]. A case study provided by Wiedemann and Jantzen [51] for Daimler-Benz AG shows that complete engine mock-ups can be fabricated by RP technique at one fifth of the cost as compared to traditional methodologies. As an example of application in medical field, the possibility of viewing and physically handling the precise geometry before surgery enables the surgeon to obtain three dimensional anatomical information as well as a solid product on which the proposed surgery can be simulated [52],[53].

Many engineering assisted surgery related publications discuss the use of bio-models generated through RP for diagnostics operation planning and preparation of implants in a virtual environment [54],[55],[56]. Some studies have been conducted integrating CAD, FE (Finite element) analysis and RP techniques for direct manufacturing of customized implant model [57]. These studies demonstrate that application of RP in surgery reduces the overall cost by reducing the theatre time and part preparation time. The inherent porosity of many products produced by RP is advantageous for construction of individual, patient-specific scaffolds[58]. Initially, RP systems have not been designed for the production of end use parts. However, design freedom and no tooling requirement with RP enables economically viable production [59],[60]. Manufacturing of end-use products using RP techniques directly from CAD model is now known as rapid manufacturing (RM)[61].RM is beneficial for the industry in terms of reducing the production equipment requirement and time period for fabrication. Multi-layer printed circuit board (PCB) can be conveniently fabricated by RP technology like SGC (solid ground curing)[62].

Although direct manufacturing of metal parts with RP is not well developed, indirect methods have been found feasible through the combination of RP and metal casting. Such type of integration gives rise to new application of RP in generating tools which are capable of forming several thousand or even millions of parts before final wear out occurs is known as rapid tooling (RT). RT is considered as natural extension of RP and is typically used to describe a process which either uses a RP model as a pattern to create a mould quickly or uses the RP process directly to fabricate a tool [63],[64]. RT methods can be classified into direct and indirect tooling categories. Indirect RT requires some kind of master pattern which can be made by any RP process. Today, almost all commercialized RP processes, selective laser sintering (SLS), stereo lithography (SL), fused deposition modelling (FDM), inkjet plotting, 3D printing (3D-P), solid ground curing (SGC), multi-jet modelling (Actua) and laminated object manufacturing (LOM) have been employed to produce patterns with varying success[65],[66],[67]. Direct RT, as the name suggests, involves manufacturing a tool cavity directly by the use of RP system; hence, eliminates the intermediate step of generating a pattern[68],[69].

## 2.2 Research and development in FDM

The development of key properties such as dimensional accuracy, surface roughness and the mechanical properties of RP parts is crucial to evolving RP applications to produce functional parts rather than only producing prototypes and to minimizing any excessive post-processing.

### 2.2.1 Dimensional accuracy

RP technology has significantly contributed to manufacturing industry, particularly by reducing the time to produce prototype parts and improving the capability to visualize part geometry. The physical prototype provides the ability for earlier detection and minimizing design errors and the capability to compute mass properties of components and assemblies. Dimensional accuracy of RP systems is still a significant obstacle preventing RP technology moving towards becoming a primary production process[70].

Also, dimensional accuracy is extremely important in any product development cycle as it directly affects part functionality. The relative importance of the accuracy of various part features is attainable from designer defined tolerances [71]. Dimensional accuracy can be defined as the deviation of the geometry from the progenitor CAD model to the real part. The thermoplastic ABS material used in FDM machines experiences a volume change when it is heated and then extruded onto a build platform[72]. RP parts tend to shrink from their given dimensions in the CAD model according to the heating and cooling processes during depositing of the layers. Consequently, after producing an RP part, it become smaller or loses its desired dimension as designed in 3D CAD. Most rapid prototyping systems use the de-facto standard STL CAD file format of solid representation to define the solid parts to be built. However, STL files pose the problems of dimension, form and surface errors resulting from approximation of three dimensional surfaces by triangular facets. Although, a large number of facets can be used to reduce these errors, doing so will result in a large data file and longer part build time. Errors that occur during the building are mainly in the manufacturing control factor setups. Different parameter setups will generate different machining accuracy and build times[73] .

RP models can suffer from warpage. Hence the RP user must consider the linear dimensional inaccuracy and warpage of RP models when considering possible applications for the RP parts. In RP technology advancement, dimensional accuracy became a key characteristic to be studied in both academic and industrial fields since the emergence of RP systems. dimensional accuracy of RP systems is still a significant obstacle preventing RP technology moving towards becoming a primary production process[74]. Dimensional accuracy is extremely important in any product development cycle as it directly affects part functionality. Similarly, the overall inaccuracy of the parts being built by RP technology has been one of the major challenges that need to be overcome[75]. Errors due to shrinkage and warpage dominate the inaccuracy of the part. The relative importance of the accuracy of various part features is attainable from designer defined tolerances. In RP system advances, several methodologies were applied to improve the dimensional accuracy of parts. Process planning of RP systems, such as data file correction, slicing data improvement, support structure generation and path planning has been investigated to improve the parts accuracy.

**O.A. Mohammed et al**[76] studied a methodology for an effective FDM process parameter optimization using I-optimal design and the mathematical models were developed to describe the relationship between input parameters and dimensional accuracy. They concluded from this work results from statistical analysis have proved that the developed regression models can describe the relation- ship between input parameters and dimensional accuracy with a 95% confidence interval, The parameters (layer thickness, air gap, build orientation, road width, and number of contours) show a significant effect on percentage change in length. It was observed that the percentage change in width of the part decreases linearly with decrease in layer thickness, air gap, road width, and number of contours. With an increase in layer thickness and number of contours from low to high level, percentage change in thickness also increases. However, the latter decreases with the increase in air gap, raster angle, build orientation, and road width, from low level toward high level.

**M.N. Sudin et al**. [43] This research investigates the dimensional accuracy of parts produced using the additive manufacturing method of Fused Deposition Modeling (FDM). They concluded that for fabricating a circular shape part, the nominal value must be set, over sizes than the intended dimension as to compensate its negative dimensional deviation. This shows that FDM machine is less accurate in producing a circular shape part such as cylindrical, sphere and hole as the majority of them are out of the machine's tolerance. It can be said that part features and its dimension will influence the dimensional accuracy of FDM parts.

### 2.2.2 Surface roughness (Ra)

The surface finish of parts obtained through RP process is highly important, especially in cases where the parts come in contact with other elements or materials in their service life, for example moulds made up of components manufactured by RP processes.

**N.H.Tran et al.**[77] Analyzed the influence of factors such as materials (filament diameter and properties), printing condition (nozzle diameter, atmosphere and pre-heating). Machine specifications (rigidity, accuracy, functions, static and dynamic behavior) and printing parameters (layer thickness, path width, printing speed, and path direction) on the part quality. Then, the optimal values of printing process are applied for printing the gears and shafts of the gear box with ABS and PLA materials.

**S. Dinesh Kumar et al.**[29] Examined five FDM parameters like layer thickness, air gap, raster width, contour width, raster orientation at two variable settings for building test parts. Full factor design was used in this study to conduct an experimentation plan to determine the optimum parameters settings that affect the output characteristic response i.e., surface roughness (Ra). they affirm that not all FDM parameters have impact on the Surface roughness; also they found that Negative air gap at (-0.01 mm) and layer thickness at (0.254 mm) or raster width at (0.508 mm) can be used to reduce surface roughness. Use small layer thickness to increase Surface Quality.

Using the optimal part orientation is vital to reduce support material, which will lead to reduce building time and improve the surface finish.

**Y.S. Dambatta et al.**[78] studied the effect of process parameters which including layer thickness and deposition on surface roughness of FDM prototypes. An ANFIS prediction model was developed to obtain the surface roughness in the FDM parts using the main critical process parameters that affects the surface quality. The experimental response shows that the process parameters deeply affects the surface quality in the FDM prototypes. It was also observed that the ANFIS model constructed for predicting the surface roughness in the FDM prototypes has an accuracy of about 93.34%.

**G.S. Bual et al.** [79] Found that there are various methods to improve surface finish of FDM parts. The surface finish can be improved by choosing suitable build orientation of the part. It can also be increased by reducing the layer thickness of build material. However, it will increase the build time. It has been found that the surface finish can also be improved by using some post processing techniques. Out of post processing techniques, chemical treatment has been used successfully to produce a very good surface finish.

### 2.2.3 Tensile strength

**O.A. Mohammed et al**[80] studied influence of critical FDM parameters-layer thickness, air gap, raster angle, build orientation, road width, and number of contours-are studied using Q-optimal response surface methodology. Their effects on build time feedstock material consumption and dynamic flexural modulus are critically examined. This study concluded that the most effective parameters on build time, feedstock material consumption and dynamic flexural modulus are found to be layer thickness, air gap, build direction and number of contours. However, raster angle and road width are less effective on build time and feedstock material consumption. Dynamic flexural modulus improved significantly using thick layers, zero air gap and 10 contours.

**D. Cristian et al.**[81] Evaluate the tensile properties of 3D printed components produced using a commercial 3D printer by performing standard tensile tests and to assess the influence of the technological parameters upon mechanical proprieties of printed specimens, considering different printing directions, infill rates and infill patterns. The influence of raster angles is tested through the designed specimens with different transverse plane, they are printed by placing in different angle, including 0°, 30°, 45° and 90°. Specimens with an infill rate varying from 20% to 100% and six different infill patterns have been tested. They concluded that the mechanical properties of ABS specimens fabricated by fused deposition modeling display are significantly influenced not only by the infill rates as expected, but also about the printed pattern of different layers and their orientation, the effect of the void geometry on the local stresses and strains will affect the macro scale mechanical behavior of the material.

**F. Rayegani et al.**[82] Determined the functional relationship between process parameters and tensile strength for the fused deposition modelling (FDM) process using the group method for data modelling for pre- diction purposes. An initial test was carried out to determine whether part orientation and raster angle variations affect the tensile strength. It was found that both process parameters affect tensile strength response. Further experimentations were carried out in which the process parameters considered were part orientation, raster angle, and raster width and air gap. The process parameters and the experimental results were submitted to the group method of data handling (GMDH), resulting in predicted output, in which the predicted output values were found to correlate very closely with the measured values. Using differential evolution (DE), optimal process parameters have been found to achieve good strength simultaneously for the response. The mathematical model of the response of the tensile strength with respect to the process parameters comprising part orientation, raster angle, raster width and air gap has been developed based on GMDH, and it has been found that the functionality of the additive manufacturing part produced is improved by optimizing the process parameters. The results obtained are very promising, and hence, the approach presented in this paper has practical application for the design and manufacture of parts using additive manufacturing technologies.

**J.M. Chacon et al.**[83] Studied the effect of build orientation, layer thickness and feed rate on the mechanical performance of PLA samples manufactured with a low cost 3D printer. Tensile and three- point bending tests are carried out to determine the mechanical response of the printed specimens. From this study they concluded that: on-edge samples showed the optimal mechanical performance in terms of strength, stiffness and ductility, ductility decreased as layer thickness increased, In upright samples, tensile and flexural strength decreased as the feed rate increased, and If minimum printing time is desired: high layer thickness and high feed rate are recommended.

## 2.3 Literature summary

This chapter reviewed several past experiments, different optimization approaches, and modeling technique that have been carried out by many researchers on FDM. For the sake of simplicity, it is divided into three main sections. In section 2.2.1, reviewed various experiments conducted by some researcher on dimensional accuracy of parts printed on FDM machine have been discussed, In Section 2.2.2 reviews the literature on optimization of surface roughness using Taguchi method and Response surface method Section 2.2.3 reviews the literature that have been carried out on optimization of processes parameters for greater tensile strength.

From the study of research papers on FDM, it is found that different process parameters for improving quality of printed part like, DA, Ra and UTS etc., different optimization technique were used in single or by hybrid with other technique.

## 2.4 Gaps in literature review

Some gaps are identified on the basis of which aim for further study has been decided. Some are

- Since this technology is resent Very few researchers are reported on usage of the Taguchi method in FDM for single and multi-objective optimization purpose.
- insufficient work has been done for optimization of flash forge creator process parameters for certain materials.
- Less work has been reported on optimization of FDM process using Taguchi methods.

# Chapter 3
# Materials and methods

## 3.1 Flash forge creator pro machine specification

Flash forge creator pro as shown in Figure 3.1, was used to produce the specimens. This machine is developed and marketed by Stratasys. The machine has large build chamber volume (227x148x150mm). It incorporates multiple materials like ABS, PLA and uses Water Works soluble support for ABS. Support material use can be easily breakaway by hand. It can build part in three available layer height that are 0.180mm, 0.290mm and 0.40mm. The creator pro has an enclosure and two fans blowing air out of the box when the nozzle fan is activated. A heated bed is featured as well as a double extruder configuration.


Figure 3.1 Flash forge creator pro

The machine is equipped with Insight software that assists the user to adjust the variable parameters in building part specification. FDM Insight software will then read the STL format to allow the user to modify the file to confirm to the building specification to create tool path-filling parameters. As shown in figure these parameters governing the most basic control of the print, such as layer height, print quality, infill density, or orientation. Others give full control over all the parameters such as infill pattern, support location, shell thickness, printing speed, and many more.

Table 3.1 FDM machine specification

| Printing specification | |
|---|---|
| **Number of extruder** | 2 |
| **Print technology** | Fused filament fabrication |
| **Screen** | LCD Panel |
| **Build volume** | 227×148×150mm |
| **Layer resolution** | 0.05-0.4mm |
| **Build precision** | ±0.2mm |
| **Positioning precision** | Z axis 0.0025mm;XY axis 0.011mm |
| **Filament diameter** | 1.75mm(±0.07) |
| **Nozzle diameter** | 0.4mm |
| **Build speed** | 10-200mm/sec |
| **Software** | Flash print |
| **AC input** | 100V-240V/4.5A-2.5A |
| **Connectivity** | USB Cable, SD Card |
| **NET Weight** | 14.8kg |

## 3.2 ABS Material

**Acrylonitrile Butadiene Styrene (ABS**) chemical formula (C8H8· C4H6·C3H3N)n) is a common thermoplastic. It used to make light, rigid, molded products such as piping (for instance Plastic Pressure Pipe Systems), musical instruments (most notably recorders and plastic clarinets), golf club heads (used for its good shock absorbance), automotive body parts, wheel covers, enclosures, protective head gear, buffer edging for furniture and joinery panels, and toys, including Lego brick.

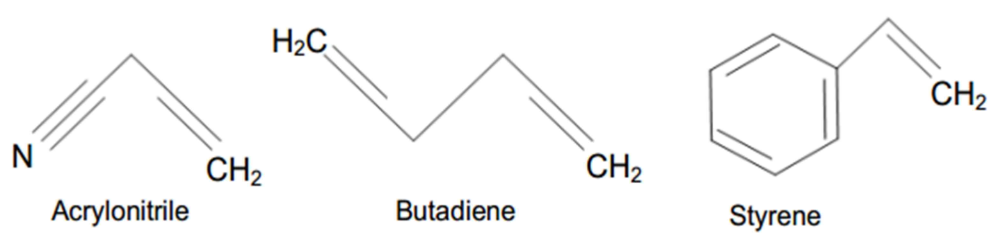


Figure 3.2 Monomers in ABS polymer

ABS is a copolymer made by polymerizing styrene and acrylonitrile in the presence of polybutadiene. The proportions can vary from 15 to 35% acrylonitrile, 5 to 30% butadiene and 40 to 60% styrene. The result is a long chain of polybutadiene crisscrossed with shorter chains of poly(styrene-co-acrylonitrile). The nitrile groups from neighboring chains, being polar, attract each other and bind the chains together, making ABS stronger than pure polystyrene. The styrene gives the plastic a shiny, impervious surface. The butadiene, a rubbery substance, provides resilience even at low temperatures. ABS can be used between -25 and 60 °C. The properties are created by rubber toughening, where fine particles of elastomer are distributed throughout the rigid matrix.it can also be recycling.

### 3.2.1 Properties of ABS plastic

The advantage of ABS is that this material combines the strength and rigidity of the acrylonitrile and styrene polymers with the toughness of the polybutadiene rubber. The most important mechanical properties of ABS are impact resistance and toughness. The table given below shows the main properties of ABS.

Table 3.2 Properties of ABS

| **Property** | **Extruded** | **Moulded** | **Unit** |
|---|---|---|---|
| **Physical property** | | | |
| **Density** | 0.350-1.26 | 1.02-1.17 | g/cm3 |
| **Moisture Absorption at Equilibrium** | 0.150 - 0.200 | 0.000 - 0.200 | % |
| **Viscosity** | 155000 - 255000 (Temperature 240-260°C) | 1.16e+6-1.52e+6 (Temperature 240-260°C ) | Cp |
| **Linear Mould Shrinkage** | 0.00240 - 0.0120 | 0.00200 - 0.00900 | cm/cm |
| **Mechanical property** | | | |
| **Hardness Rockwell R** | 90.0 - 121 | 68.0 - 115 | |
| **Tensile Strength, Ultimate** | 27.0 - 52.0 | 28.0 - 49.0 | MPa |
| **Tensile Strength, Yield** | 20.0 - 62.0 | 13.0 - 65.0 | MPa |
| **Modulus of elasticity** | 1.52-6.10 | 1.00-2.65 | GPa |
| **Elongation at Yield** | 0.620 - 30.0 | 1.70 - 6.00 | % |
| **Flexural Modulus** | 1.20 - 5.50 | 1.61 - 5.90 | GPa |
| **Flexural Yield Strength** | 28.3 - 81.0 | 40.0 - 111 | MPa |
| **Chirpy Impact, Notched** | 0.900 - 5.00 | 0.400 - 14.0 | J/cm² |
| **Izard Impact, Notched** | 0.380 - 5.87 | 0.100 - 6.40 | J/cm |
| **Thermal properties** | | | |
| **Thermal Conductivity** | 0.150 - 0.200 | 0.128 - 0.200 | W/m-K |
| **Coefficient of thermal Expansion, linear** | 68.0 - 110 | 0.800 - 155 | µm/m-°C |
| **Glass Transition Temperature** | 108 - 109 | 105 - 109 | °C |

## 3.3 Experimentation setup: Selection of parameter

Some of the main flash forge variable parameters are considered in this research to evaluate the correlation between these parameters and the proposed response characteristics. these parameters are described as follow.

**Layer height**

It is recognized as the height of deposited slice from the FDM nozzle. Layer height decides on how high each layer will be, in other words how much the extruder is translated in Z direction for each layer shift.

**Infill**

Infill pattern in 3D printing refers to the structure that is printed inside the model. By using slicing software, an infill pattern for an object can be defined in various percentage and shapes. Infill patterns influence the print time, weight, print quality, object strength and its mechanical properties. For this study the values of 15%,30%and 45% were considered. For printing solid patterns, an infill route must be defined that completely fills the desired area, while giving a uniform print quality over the area, with as little material usage as possible.

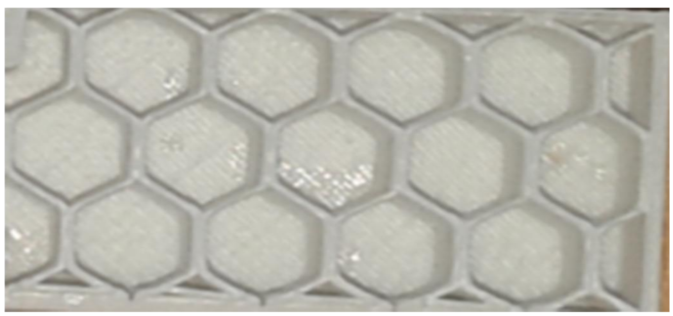

Figure 3.3 Infill pattern of part one

**Printing speed**

The printing speed is the speed which the extruder moves in X and Y direction. This is usually set between 10 mm/sec and 200 mm/sec.

**Build temperature**

It is temperature of the heated nozzle and the temperature of the plastic has when it is extruded. Build temperature is one of the most important parameters to be considered during part fabrication.

Four factors layer height(A), infill density (B), build speed (C) and build temperature (D) varied each at three level, as shown in Table 3.3 are considered. Others factors are kept at fixed level as shown in Table 3.3.

Table3.3 Process parameters to be controlled

| Factors | symbol | unit | Level 1 | Level 2 | Level 3 |
|---|---|---|---|---|---|
| **Layer height** | A | mm | 0.180 | 0.290 | 0.40 |
| **Infill** | B | % | 15 | 30 | 45 |
| **Build speed** | C | mm/sec | 60 | 120 | 180 |
| **Build temperature** | D | ℃ | 220 | 240 | 260 |

## 3.4 Design of experiment

Design of experiment is a systematic and scientific way of planning the experiments, collection and analysis of data with limited use of available resource. The DOE approach helps to study many factors simultaneously and most economically by studying the effects of individual factors on the result, the best factor combination can be determined. Since design of experiment using Taguchi's provides an efficient plan to study the experiments, with minimum amount of experimentation, it was chosen for performing the FDM variable process parameters experiments. Based on selected cutting process parameters and their levels a experimental design matrix was constructed (Table 3.4) using Taguchi L9 orthogonal array (three levels-four factors) were selected depends on number of factors and their levels. Each experimental trials in the design consists of combination of different FDM parameters with different levels. It is used to measure surface roughness (Ra), dimensional accuracy (DA) and tensile strength (UTS)

Table 3.4 Experimental data obtained from the L9 orthogonal array

| **EXP. trials** | **Input parameters** | | | |
|---|---|---|---|---|
| | Laser height mm | Infill % | Build speed mm/sec | Build Temperature °C |
| **1** | 0.180 | 15 | 60 | 220 |
| **2** | 0.180 | 30 | 120 | 230 |
| **3** | 0.180 | 45 | 180 | 240 |
| **4** | 0.290 | 15 | 60 | 220 |
| **5** | 0.290 | 30 | 120 | 230 |
| **6** | 0.290 | 45 | 180 | 240 |
| **7** | 0.40 | 15 | 60 | 220 |
| **8** | 0.40 | 30 | 120 | 230 |
| **9** | 0.40 | 45 | 180 | 240 |

## 3.5 Specimen fabrication

Specimens are fabricated using Flash forge FDM machine for respective characteristic measurement. The 3D models of specimens are generated using SOLID WORK 2016 solid modeling software and exported as STL (stereo lithography) file to FDM software (Insight). Figure 3.4 is showing the specimen model on solid work.

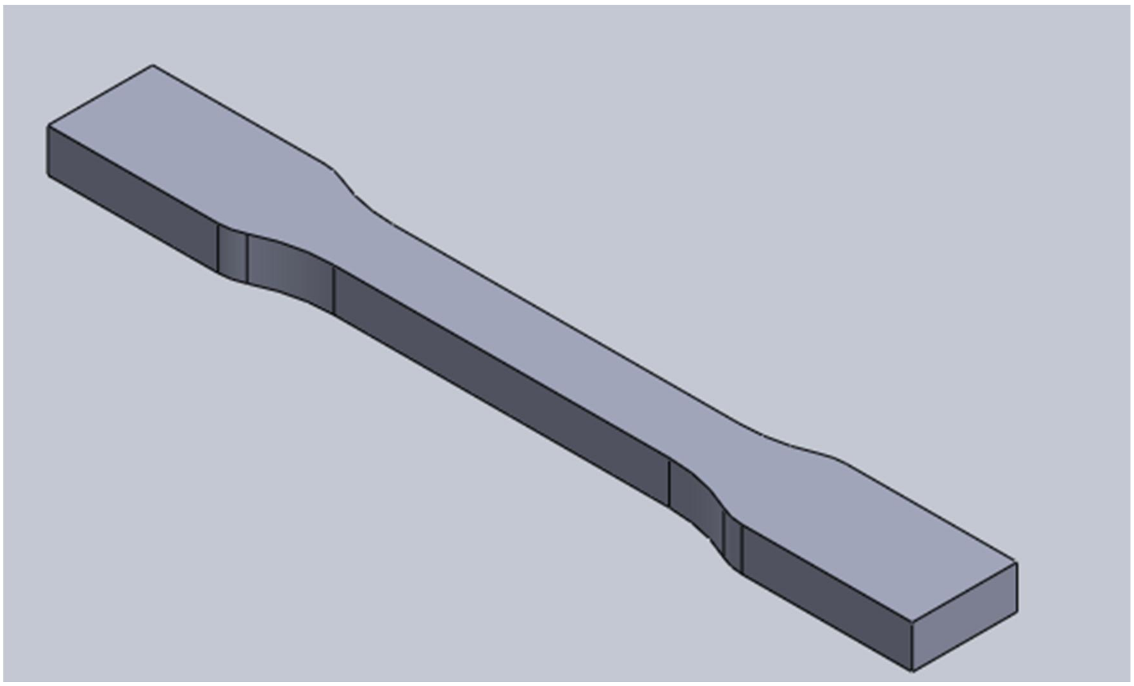

Figure 3.4 Specimen model on Solid work

STL file it is time to convert the model to an X, Y and Z based code that the printer can read, this code is called a g-code. As the 3D printer is using X, Y and Z coordinates to navigate this code is needed. The process where a. G CODE is generated in 3D printing context is called slicing. Figure 3.5 is showing the interface of the slicing software Simplify3D.

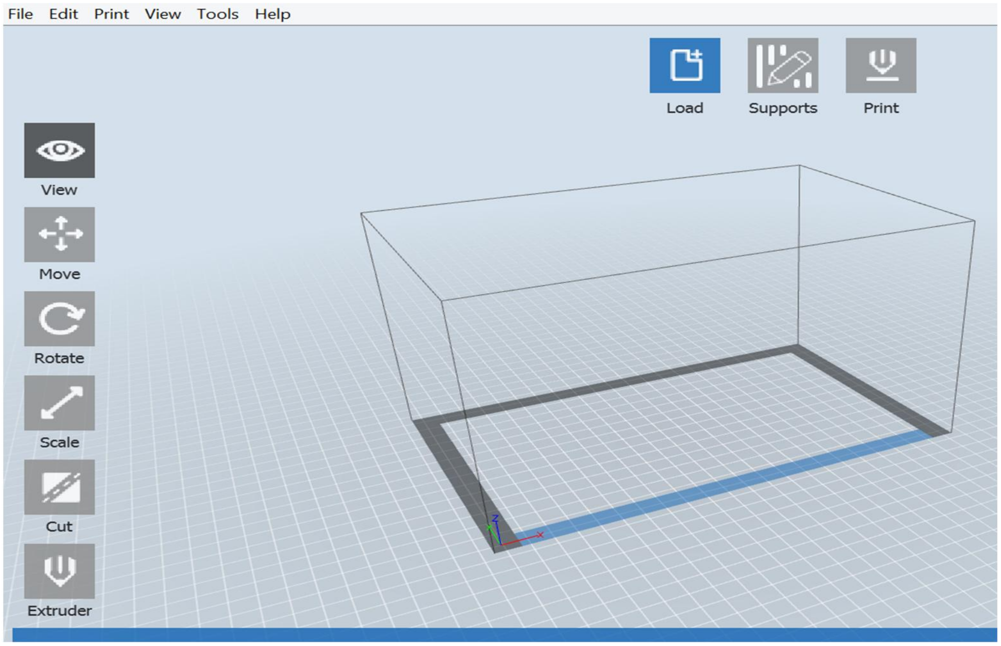


Figure 3.5 Simplify3D slicer software interface

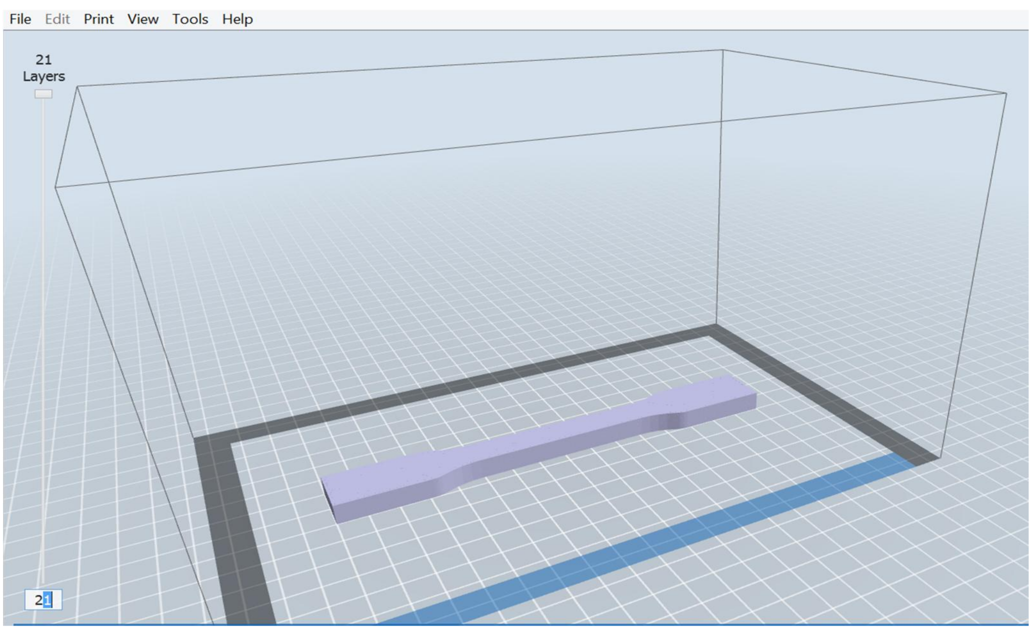


Figure 3.6 3D STL Model placed on the virtual bed in Simplify3D

The above Figure 3.6 shows the specimen placed flat on the building plate virtually in the slicing software. X, Y and Z axis directions are shown. After this, data is sent to the FDM hardware for modeling. The forming material (ABS) in the form of a flexible strand of solid material is supplied from a supply source spool to the head of the machine. One pair of wheels or rollers having a nip in between are utilized as material advance mechanism to grip a flexible strand of modeling material and advance it into a heated dispensing or liquefier head.

The material is heated above its solidification temperature by a heater (liquefier) on the dispensing head and extruded in a semi molten state on a previously deposited material onto the build platform following the designed tool path. The head is attached to the gantry that man oeuvres the head in the X and Y directions when building a part. The XY gantry assembly is located under the top hood of the machine. The entire gantry is outside of the build chamber. Only the bottom of the head protrudes into the build chamber. The build platform moves along the Z direction. The drive motion is provided to selectively move the build platform and dispensing head relative to each other in a predetermined pattern through drive signals input to the drive motors from CAD/CAM system.

For material deposition FDM uses two nozzles, one for model material deposition and other for support material deposition. These two nozzles work alternately to each other. The following figure provides the schematic description of steps entailed during part fabrication in FDM machine. The fabricated part takes the form of a laminate composite with vertically stacked layers, each of which consists of contiguous material fibers or raster with interstitial voids. Fiber-to-fiber bonding within and between layers occurs by a thermally driven diffusion bonding process during solidification of the semi-liquid extruded fiber.

Figure 3.7 Parts fabricated by FDM machine

## 3.6 Methods of Measurement and Testing

### 3.6.1 Dimensional accuracy

Dimensional accuracy is understood as degree of compatibility of basic dimensions of the obtained product with dimensions of the ideal product (nominal dimensions). The dimension of fabricated parts is measured at five different location using Varner calliper with least account of 0.02 mm. Venire calliper is a precision instrument that can be used to measure external distances accurately. For measurement purpose it has two jaws, external and internal jaws. External jaws are used to measure external dimensions like length, width and thickness. Other than these two jaws, there is depth-measuring bar used for measuring the heights or depth. For measuring length (L), width (W) and thickness (T), the specimen to be measured is placed between external jaws and they are carefully brought together. Test specimen employed for measuring dimensional accuracy is shown in Figure 3.9.

Figure 3.9 Test sample for dimensional analysis

Measurements show that measured length (L), width (W) and thickness (T) is always more than the CAD model value.

Relative change in dimensions ($\Delta W$, $\Delta T$ and $\Delta L$) can be calculated using equation 3.1. Relative change in dimensions = $(X - X_{CAD})/X_{CAD})$ ……………………………… Equation 3.1

Where, X is the measured value of length or width or thickness, $X_{CAD}$ represent the respective CAD model value.

### 3.6.2 Surface roughness (Ra)

The surface roughness was measured by using standardized surface roughness device called BELLSTONE surface tester on the flat top of the designed benchmark part. Surface roughness of each fabricated parts are measure at five different places on the top and bottom surfaces and the average values used for analysis, the unit of measure is µm. Figure 3.10 shows the BELLSTONE equipment and the fabricated part. In addition, the measurement has been performed in the direction of built layers as shown in figure.


Figure 3.10 Measurements by BELLSTONE to the parts produced by flash forge FDM

### 3.6.3 Tensile strength

The tensile strength of material is defined as the maximum stress that the material can sustain under uniaxial tensile loading. The ability of a composite material to withstand forces that pull it apart is analyzed by its tensile strength, basically stating the extent to which the material will stretch before breaking. The load-indicator zero and the plot-load-axis zero, if applicable, should be set before the specimen is placed in the grips. Then the specimen placed in the grips by proper alignment and specimen tabs should be fully engaged by closing the grips. One of the cross head is fixed at one end and other end is move uniaxial, the peak force (load at break) measured.

The tensile tests were carried out using a testometric material testing machine 350 KN maximum capacity, The cross head speed of this machine is 1mm/min and the test stops once the specimens broken. The material used for specimen preparation is ABS with a nominal thickness of 8 mm, width 12 mm and the tensile strength is calculated by dividing maximum load(load at break) with original cross sectional area(original width × original thickness).

$$Tensile\ strength\ (UTS) = \frac{Breaking\ load(Pf)}{(orignal\ cross\ sectional\ area(Ao)} \quad \text{............. .Equation 3.2}$$

Figure 3.11 shows testometric and tensile testing in order to predict the influence of FDM parameters settings on tensile strength.


Figure 3.11 Testometric Machine and tested specimen

## 3.7 Methods of analysis

To investigate the relationship between variable parameters and the outcome response, a number of analysis methods should be followed. In this research work, various analysis methodologies were used to relate the response compressively. Taguchi analysis, Signal to Noise ratio (S/N ratio) and analysis of variance (ANOVA) were used for analysis and optimization of experimental result. Main effect plots, Interaction plots, 3D Surface plots and Contour plots were also plots using Minitab (V 18.1) software to study relationship between process parameters and outcome results.

### Taguchi analysis

Taguchi analysis for dimensional accuracy, surface roughness and tensile strength were done to relate rank of various factors in terms their relative significance. Taguchi analysis were done with the help of Minitab. It clearly shows that which factor most significantly affect, which one has less effect on the response outcome respectively.

### Signal to noise ratio (S/N):

According to Taguchi method, the S/N ratio is the ratio of signal to noise where signal represents the desirable value (i.e., the mean for the output characteristics), and noise represents the undesirable value (i.e., the square deviation for the output characteristics). To evaluate quality of fabricated parts, all experimental result should be transformed into the S/N ratios. Depending on the goal of the experiment for the quality representative to be optimized, different S/N ratios can be chosen: Smaller-the better, Nominal - the best and larger- the better. In this case lower values of the dimensional accuracy and surface roughness are desirable for maintaining high cut quality. In case of tensile strength larger – the better has been chosen. According to this study The S/N ratio for mean surface roughness and dimensional inaccuracy are calculated using the smaller the-better criterion as depicted in Equation (3.3) and the larger the –better criterion as depicted in Equation (3.4) for tensile strength.

$$SNR_s = -10 \log \sum_{i=1}^{n} \frac{y_i^2}{n} \quad \text{……………………………………Equation (3.3)}$$

$$SNR_l = -10 \log \sum_{i=1}^{n} \frac{1/y_i^2}{n} \quad \text{……………………………………. Equation (3.4)}$$

Where, n is the number of experiments in the orthogonal array and $y_i$the $i_{th}$value measured.

**Analysis of variance (ANOVA)**

The results for experiments were analyzed using ANOVA for identifying the significant factors affecting the performance measures. For significance check F – value and P – value given in ANOVA table is used. The principle of the F-test and P- test is that the larger F value and smaller value for a particular parameter, the greater the effect on the performance characteristic due to the change in that process parameter. If the P- value less than 0.05 (i.e., α = 0.05, or 95% confidence level) indicate process parameters term are significant and P - Values greater than 0.1000 indicate the model terms are not significant, which implies the Lack of Fit is significant, this large could occur due to noise.

# Chapter 4
# Result and Discussion of Dimensional accuracy

## 4.1 Introduction

In this section result of Dimensional accuracy like; width, length, and thickness are analyzed and optimized using Taguchi methods. Effect of process parameters like; layer height, infill, build speed, and build temperature on dimensional accuracy of produced parts using Flash forge FDM machine are optimized using Taguchi method. Analysis of Variance, main effect plots, Interaction plots, 3D Surface plots and Contour plots for Dimensional accuracy are constructing with the help of Minitab V18.1 software, to analysis the relationship between each process parameters. Optimum setting was determined using S/N ratio.

## 4.2 Result of Dimensional accuracy

The difference between CAD model dimension and actual dimension is measured and mean results were used for Analysis purpose. The results of Dimensional accuracy (ΔW, ΔT, and ΔL) for each of 9 experiments are given in Table 4.1. S/N ration was calculated using MINITAB V18 trial software. The unit of measure is mm. In Figure (4.1 – 4.3) Bar chart plots for mean and S/N ratio shows distribution of dimensional accuracy like ΔW, ΔT, and ΔL for each experimental trial respectively

Table 4.1 Experimental result of Dimensional accuracy: ΔW, ΔT, ΔL

| Exp. trial | Factors | | | | Relative change in dimension | | | | | |
|---|---|---|---|---|---|---|---|---|---|---|
| | Layer height mm | Infill % | Build speed mm/min | Build temperature ºC | Mean ΔW | S/N ratio | Mean ΔT | S/N ratio | Mean ΔL | S/N ratio |
| 1 | 0.180 | 15 | 60 | 220 | 0.0266 | 31.5024 | 0.0075 | 42.4988 | 0.0061 | 44.2934 |
| 2 | 0.180 | 30 | 120 | 230 | 0.0156 | 36.1375 | 0.0087 | 41.2096 | 0.0061 | 44.2934 |
| 3 | 0.180 | 45 | 180 | 240 | 0.0176 | 35.0897 | 0.0106 | 39.4939 | 0.0057 | 44.8825 |
| 4 | 0.290 | 15 | 60 | 220 | 0.0048 | 46.3752 | 0.0044 | 47.1309 | 0.0056 | 45.0362 |
| 5 | 0.290 | 30 | 120 | 230 | 0.0152 | 36.3631 | 0.011 | 39.1721 | 0.0061 | 44.2934 |
| 6 | 0.290 | 45 | 180 | 240 | 0.0102 | 39.8280 | 0.0141 | 37.0156 | 0.0060 | 44.4370 |
| 7 | 0.40 | 15 | 60 | 220 | 0.0192 | 34.3340 | 0.0056 | 45.0362 | 0.0059 | 44.5830 |
| 8 | 0.40 | 30 | 120 | 230 | 0.0202 | 33.8930 | 0.01 | 40.0000 | 0.0060 | 44.4370 |
| 9 | 0.40 | 45 | 180 | 240 | 0.0199 | 34.0229 | 0.0109 | 39.2515 | 0.0061 | 44.2934 |

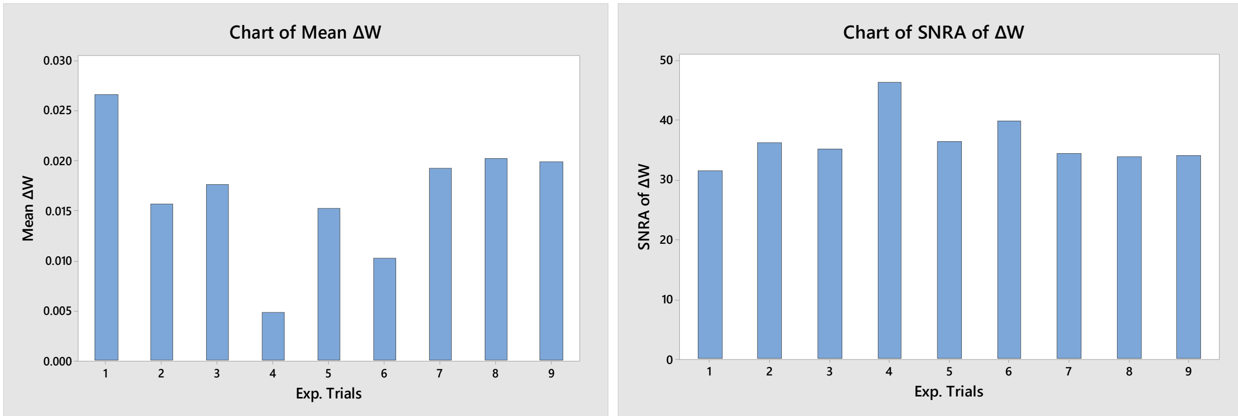


(a) (b)

Figure 4.1 Bar chart plots for mean and S/N ratio of ΔW

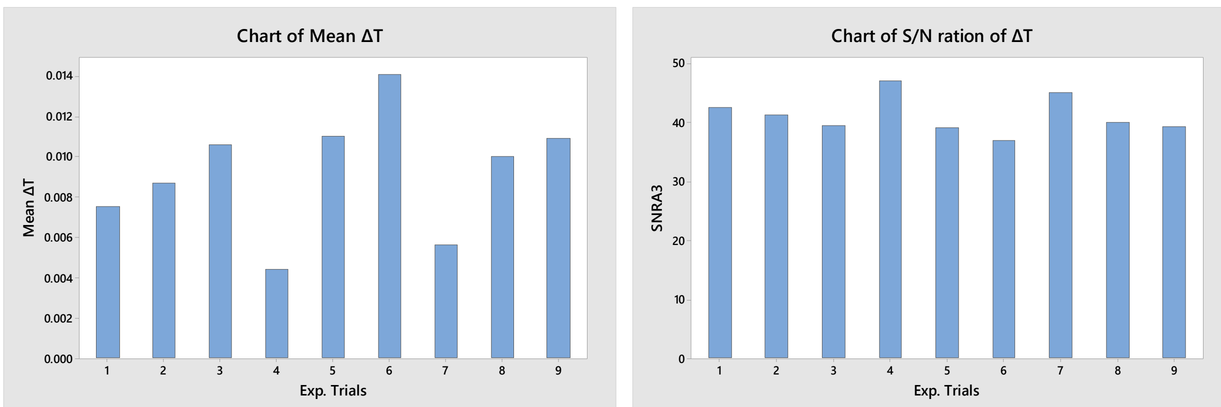


(a) (b)

Figure 4.2 Bar chart plots for mean and S/N ratio of ΔT

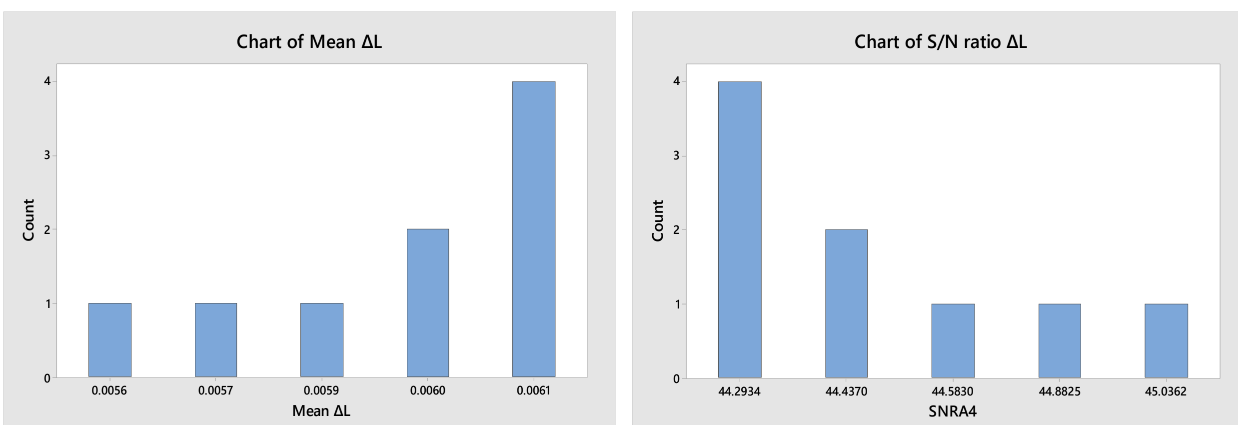


(a) (b)

Figure 4.3 Bar chart plots for mean and S/N ratio of ΔL

## 4.3 Taguchi analysis for Dimensional accuracy

Results of dimensional accuracy were analyzed using Taguchi analysis. Table 4.2 and 4.3 shows rank of various factors in terms their relative significance for relative change in dimension of width (ΔW). From the table it can be clearly observe that layer height has most significant factors, followed by build temperature, build speed and infill respectively. Table 4.2 shows response table for mean ΔW and Table 4.3 shows response table for S/N ratio of ΔW.

Table 4.2 Response table for mean ΔW

| Level | Layer height mm | Infill % | Build speed mm/min | Build temperature ºC |
|---|---|---|---|---|
| **1** | 0.01993 | 0.01687 | 0.01900 | 0.02057 |
| **2** | 0.01007 | 0.01700 | 0.01343 | 0.01500 |
| **3** | 0.01977 | 0.01590 | 0.01733 | 0.01420 |
| **Delta** | 0.00987 | 0.00110 | 0.00557 | 0.00637 |
| **Rank** | 1 | 4 | 3 | 2 |

Table 4.3 Response table for S/N ratio of ΔW

Smaller is better

| Level | Layer height mm | Infill % | Build speed mm/min | Build temperature ºC |
|---|---|---|---|---|
| **1** | 34.24 | 37.40 | 35.07 | 33.96 |
| **2** | 40.86 | 35.46 | 38.85 | 36.77 |
| **3** | 34.08 | 36.31 | 35.26 | 38.45 |
| **Delta** | 6.77 | 1.94 | 3.77 | 4.49 |
| **Rank** | 1 | 4 | 3 | 2 |

Table 4.4 and 4.5 shows rank of various factors in terms of their relative significance for relative change in dimension of thickness (ΔT). From the table it can be clearly observe that infill has most significant factors, followed by build speed, build temperature and layer height respectively.

Table 4.4 Response table for mean ΔT

| Level | Layer height mm | Infill % | Build speed mm/min | Build temperature ºC |
|---|---|---|---|---|
| **1** | 0.008933 | 0.005833 | 0.010533 | 0.009800 |
| **2** | 0.009833 | 0.009900 | 0.008000 | 0.009467 |

| | | | | |
|---|---|---|---|---|
| **3** | 0.008833 | 0.011867 | 0.009067 | 0.008333 |
| **Delta** | 0.001000 | 0.006033 | 0.002533 | 0.001467 |
| **Rank** | 4 | 1 | 2 | 3 |

Table 4.5 Response table for S/N ratio of ΔT

Smaller is better

| Level | Layer height mm | Infill % | Build speed mm/min | Build temperature ºC |
|---|---|---|---|---|
| **1** | 41.07 | 44.89 | 39.84 | 40.31 |
| **2** | 41.11 | 40.13 | 42.53 | 41.09 |
| **3** | 41.43 | 38.59 | 41.23 | 42.21 |
| **Delta** | 0.36 | 6.30 | 2.69 | 1.90 |
| **Rank** | 4 | 1 | 2 | 3 |

Table 4.6 and 4.7 shows rank of various factors in terms of their relative significance for relative change in dimension of length (ΔL). It can be observe that build temperature has most significant factor affecting relative change of length followed by infill, build speed and layer height respectively.

Table 4.6 Response table for mean ΔL

| Level | Layer height mm | Infill % | Build speed mm/min | Build temperature ºC |
|---|---|---|---|---|
| **1** | 0.005967 | 0.005867 | 0.006033 | 0.006100 |
| **2** | 0.005900 | 0.006067 | 0.005933 | 0.006000 |
| **3** | 0.006000 | 0.005933 | 0.005900 | 0.005767 |
| **Delta** | 0.000100 | 0.000200 | 0.000133 | 0.000333 |
| **Rank** | 4 | 2 | 3 | 1 |

Table 4.7 Response table for S/N ratio of ΔL

Smaller is better

| Level | Layer height mm | Infill % | Build speed mm/min | Build temperature ºC |
|---|---|---|---|---|
| **1** | 44.49 | 44.64 | 44.39 | 44.29 |
| **2** | 44.59 | 44.34 | 44.54 | 44.44 |
| **3** | 44.44 | 44.54 | 44.59 | 44.79 |
| **Delta** | 0.15 | 0.30 | 0.20 | 0.49 |

| Rank | 4 | 2 | 3 | 1 |
|---|---|---|---|---|

## 4.4 Analysis of variance for Dimensional accuracy: ΔW, ΔT, ΔL

The results for dimensional accuracy were analyzed using ANOVA for identifying the significant factors affecting the performance measures. In Table 4.8 and Table 4.9 shows, result of analysis of variance (ANOVA) for the mean and S/N ratio of relative change in width (ΔW) at 95% confidence interval respectively. For significance check F – value and P – value given in ANOVA table is used. The principles of the F-test and P- test is that the larger F value and smaller value for a particular parameter, the greater the effect on the performance characteristic due to the change in that process parameter. If the P- value less than 0.0500 (i.e., $\alpha = 0.05$, or 95% confidence level) indicate process parameters term are significant. ANOVA table for mean and S/N ratio of relative change in width (ΔW) shows that P – value 0.015 and 0.0185 respectively which is less than 0.05 for layer height, this shows that layer height has most significant factor that affects the mean and S/N ratio relative change in width (ΔW).

Table 4.8 Analysis of Variance for means ΔW

| Source | DF | Adj SS | Adj MS | F-Value | P-Value |
|---|---|---|---|---|---|
| **Layer height** | 2 | 0.000231 | 0.000116 | 2.31 | 0.015 |
| **Infill** | 2 | 0.000008 | 0.000004 | 0.08 | 0.215 |
| **Build speed** | 2 | 0.000109 | 0.000027 | 1.02 | 0.118 |
| **Build temperature** | 2 | 0.000196 | 0.000073 | 1.65 | 0.048 |
| **Error** | 4 | 0.000200 | 0.000050 | | |
| **Total** | 12 | 0.000744 | | | |

Table 4.9 Analysis of Variance for S/N ratio of ΔW

| Source | DF | Adj SS | Adj MS | F-Value | P-Value |
|---|---|---|---|---|---|
| **Layer height** | 2 | 94.755 | 47.377 | 2.65 | 0.0185 |
| **Infill** | 2 | 2.661 | 1.331 | 0.07 | 0.629 |
| **Build speed** | 2 | 19.331 | 14.326 | 0.98 | 0.474 |
| **Build temperature** | 2 | 47.685 | 23.854 | 1.57 | 0.039 |
| **Error** | 4 | 16.453 | 7.863 | | |
| **Total** | 12 | 183.885 | | | |

In Table 4.10 and Table 4.11 shows, result of analysis of variance (ANOVA) for the mean and S/N ratio of relative change in thickness (ΔT) at 95% confidence interval respectively. ANOVA table for mean and S/N ratio of relative change in thickness (ΔT) shows that P – value 0.035 and

0.046 respectively that is less than 0.05 for infill density, this shows that infill density has most significant factor that affects the mean and S/N ratio relative change in thickness (ΔT).

Table 4.10 Analysis of Variance for means ΔT

| Source | DF | Adj SS | Adj MS | F-Value | P-Value |
|---|---|---|---|---|---|
| **Layer height** | 2 | 0.000006 | 0.000003 | 0.73 | 0.536 |
| **Infill** | 2 | 0.000059 | 0.000029 | 7.45 | 0.035 |
| **Build speed** | 2 | 0.000036 | 0.000017 | 2.59 | 0.069 |
| **Build temperature** | 2 | 0.000009 | 0.000005 | 0.98 | 0.462 |
| **Error** | 4 | 0.00006 | 0.000004 | | |
| **Total** | 12 | 0.00017 | | | |

Table 4.11 Analysis of Variance for S/N ratio of % ΔT

| Source | DF | Adj SS | Adj MS | F-Value | P-Value |
|---|---|---|---|---|---|
| **Layer height** | 2 | 3.150 | 1.575 | 0.32 | 0.746 |
| **Infill** | 2 | 64.530 | 32.265 | 6.47 | 0.046 |
| **Build speed** | 2 | 31.254 | 15.987 | 3.15 | 0.124 |
| **Build temperature** | 2 | 4.548 | 1.951 | 0.38 | 0.705 |
| **Error** | 4 | 9.943 | 4.986 | | |
| **Total** | 12 | 113.425 | | | |

In Table 4.12 and Table 4.13 shows, result of analysis of variance (ANOVA) for the mean and S/N ratio of relative change in length (ΔL) at 95% confidence interval respectively. ANOVA table for mean and S/N ratio of relative change in length (ΔL) shows that P – value 0.042 and 0.037 respectively that is less than 0.05 for build temperature, this shows that build temperature has the most significant factor that affects the mean and S/N ratio relative change in length (ΔL).

Table 4.12 Analysis of Variance for means ΔL

| Source | DF | Adj SS | Adj MS | F-Value | P-Value |
|---|---|---|---|---|---|
| **Layer height** | 2 | 0.002559 | 0.001279 | 0.02 | 0.978 |
| **Infill** | 2 | 0.084187 | 0.084187 | 1.10 | 0.371 |
| **Build speed** | 2 | 0.057462 | 0.028731 | 0.50 | 0.618 |
| **Build temperature** | 2 | 0.124678 | 0.62339 | 1.48 | 0.042 |
| **Error** | 4 | 0.569183 | 0.056918 | | |
| **Total** | 12 | 0.838069 | | | |

Table 4.13 Analysis of Variance for S/N ratio of ΔL

| Source | DF | Adj SS | Adj MS | F-Value | P-Value |
|---|---|---|---|---|---|

| | | | | | |
|---|---|---|---|---|---|
| **Layer height** | 2 | 2 | 0.0174 | 0.00871 | 0.01 |
| **Infill** | 2 | 1.5754 | 1.57536 | 1.22 | 0.338 |
| **Build speed** | 2 | 1.0547 | 0.52737 | 0.48 | 0.632 |
| **Build temperature** | 2 | 2.6546 | 1.32730 | 1. 44 | 0.037 |
| **Error** | 4 | 10.9714 | 1.09714 | | |
| **Total** | 12 | 16.2735 | | | |

## 4.5 Main effect and interaction plot for mean and S/N ratio:  ΔW, ΔT, ΔL

Figure 4.4 shows main effect plot for mean and S/N ratio of relative change in width (ΔW). From main effect plot for mean relative change in width (ΔW), it is clearly shows that ΔW decrease with increasing layer height until 0.29 mm after this point it start to increase. In other case, increasing infill rate will insignificant effect on ΔW.  ΔW decrease with increasing build speed but after 12 mm/sec it start to increase. ΔW decrease with increasing build temperature. From main effect plot for S/N ratio of ΔW, it is clearly indicates that the S/N ratio of ΔW increases with increasing layer height until 0.29 mm after this point it start to decrease. In other case S/N ratio of % ΔW decreases with increasing infill rate. S/N ratio of ΔW increase with increasing build speed but after 12 mm/sec, it starts to decrease. S/N ratio of ΔW increase with increasing builds temperature. Figure 4.5 shows the interaction between process parameters on the relative change in width (ΔW).

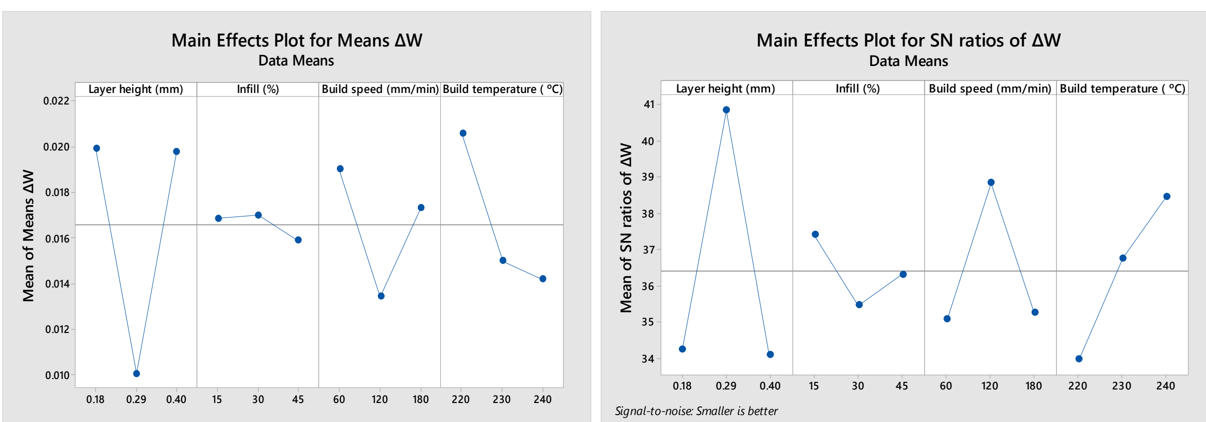


(a) (b)

Figure 4.4 Main effect plot for mean and S/N ratio of  ΔW

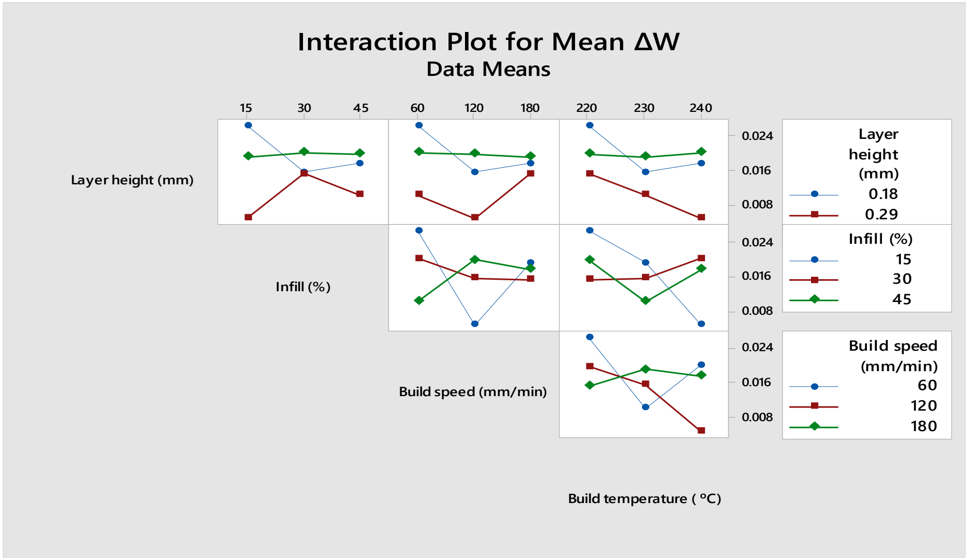


Figure 4.5 Interaction plot for mean ΔW with all process parameters

Figure 4.6 shows main effect plot for mean and S/N ratio of relative change in thickness (ΔT). From main effect plot for mean ΔT, it is clearly shows that mean relative change in thickness (ΔT) increases with increasing layer height until 0.29 mm after this point it start to decrease. In other case, increasing infill rate will increase ΔT dynamically. ΔT decrease with increasing build time but after 12 mm/sec, it starts to increase. ΔT decrease with increasing build temperature. From main effect plot for S/N ratio of ΔT, it is clearly indicates that the S/N ratio of ΔT remain constant with increasing layer height until 0.29 mm after this point, it starts to increase. In other case S/N ratio of ΔT decreases dynamically with increasing infill rate. S/N ratio of ΔT increase with increasing build speed but after 12 mm/sec, it starts to decrease. Increasing builds temperature will increase S/N ratio of ΔT. Figure 4.7 shows the interaction between process parameters on the ΔT.

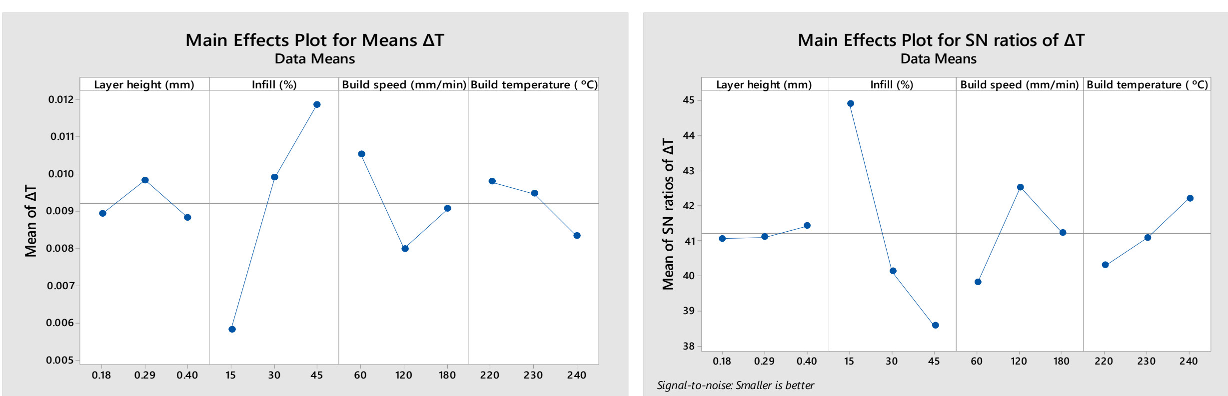


(a) (b)

Figure 4.6 Main effect plot for mean and S/N ratio of ΔT

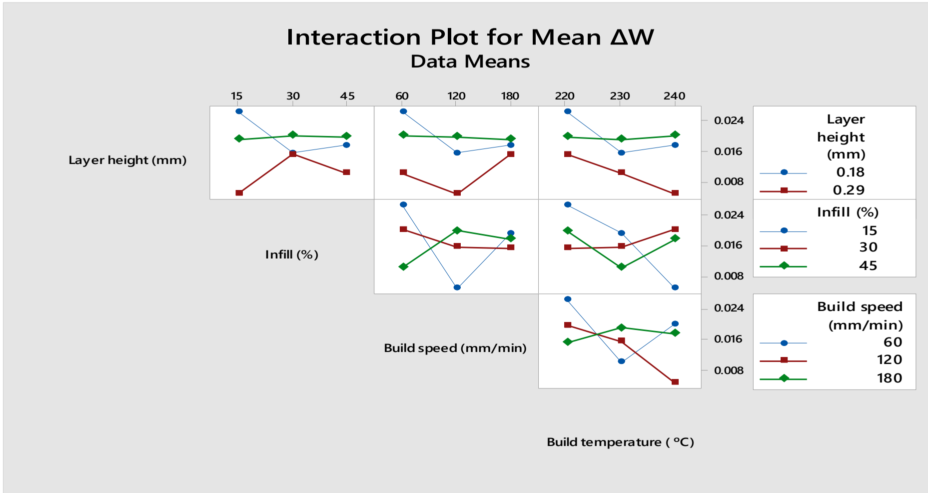


Figure 4.7 Interaction plot for mean ΔT with all process parameters

Figure 4.8 shows main effect plot for mean and S/N ratio of relative change in length (ΔL). From main effect plot for mean relative change in length (ΔL), it is clearly shows that ΔL decreases with increasing layer height until 0.29 mm after this points, it starts to increases. In other case, increasing infill rate will increase ΔL until 30%, after this point, it starts to decrease. As increasing build speed, ΔL will decrease. Relative change in length (ΔL) decrease with increasing builds temperature. From main effect plot for S/N ratio of % ΔL, it is clearly indicates that the S/N ratio of ΔL increase with increasing layer height until 0.29 mm after this points, it starts to decrease. In other case, increasing infill rate will decrease ΔL until 30%, after this point, it starts to increase. As increasing build speed, ΔL will increase. Relative change in length (ΔL) increase dynamically with increasing builds temperature. Figure 4.9 shows the interaction between process parameters on the ΔL.

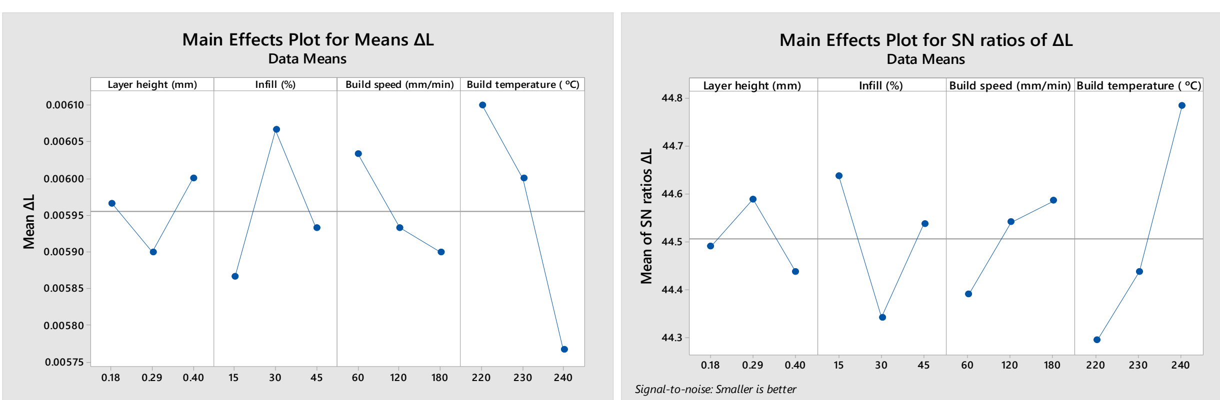


(a) (b)

Figure 4.8 Main effect plot for mean and S/N ratio of ΔL

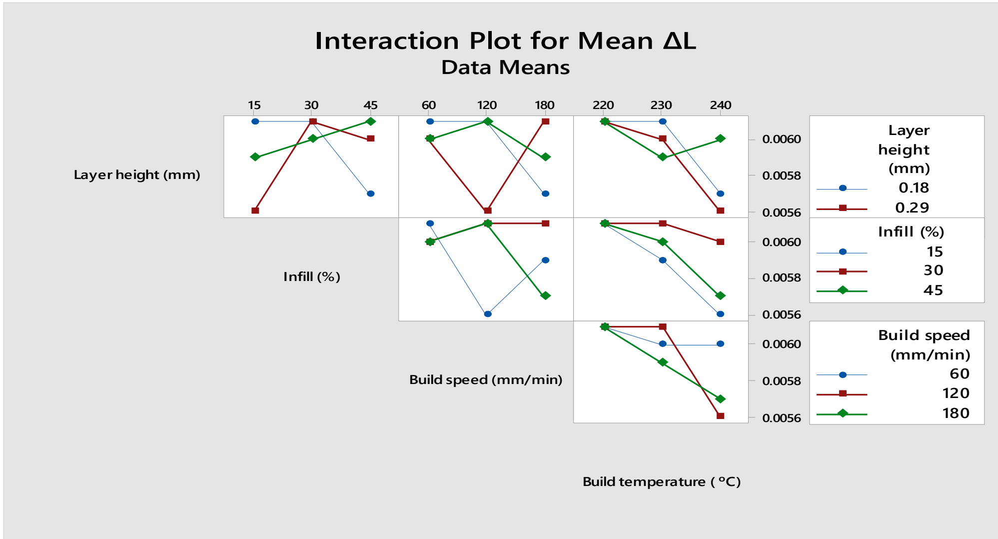


Figure 4.9 Interaction plot for mean ΔL with all process parameters

## 4.6 3D Surface and Contour plot for Dimensional accuracy

3D surface and contour graphs are, plot for dimensional accuracy against Layer height, Infill, Build speed and Build temperature, constructing to analysis the relationship between each process parameters. Figure 4.10 (a-b) shows 3D surface and contour plot of the interaction analysis between infill and layer height for mean ΔW. From this plot, it is clearly show that the lower ΔW is observed at layer height between 0.25 mm and 0.35 mm and at Infill between 40 % and 45 %. At lower layer height and Infill, the ΔW was higher. Therefore, optimum means ΔW can be obtained at the middle of layer height and higher infill rate value.

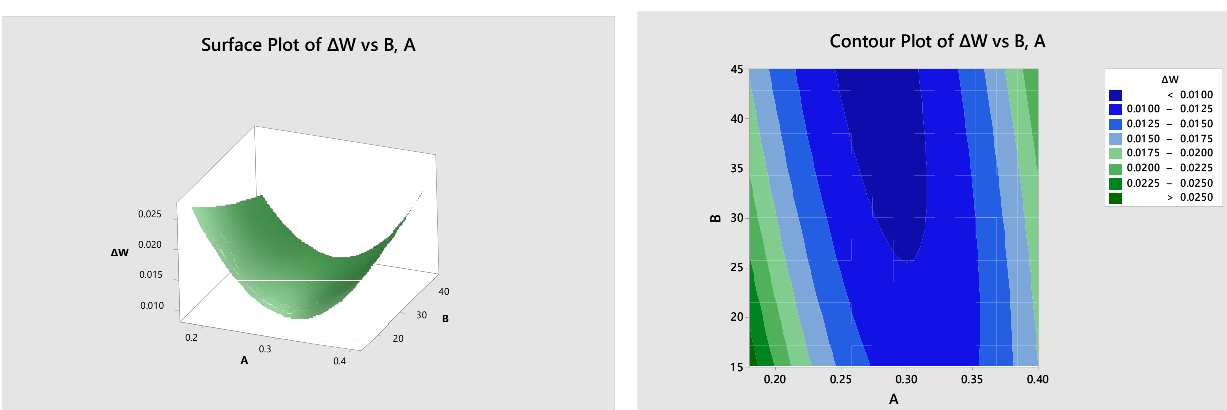


(a) (b)

Figure 4.10 (a-b): 3D Surface and contour plots of **%** ΔW against Infill(B) and Layer height(A)

Figure 4.11 (a-b) shows 3D surface and contour plot of the interaction analysis between infill and layer height for S/N ratio of ΔW. From this plot, it is clearly show that the higher S/N ratio of ΔW is observed at layer height between 0.25 mm and 0.35 mm, and at Infill between 15 % and 45 %, this mean that infill rate has insignificant effect on S/N ratio of ΔW. At lower layer height and Infill, the ΔW was low. It can be also observe that at higher layer height and Infill.

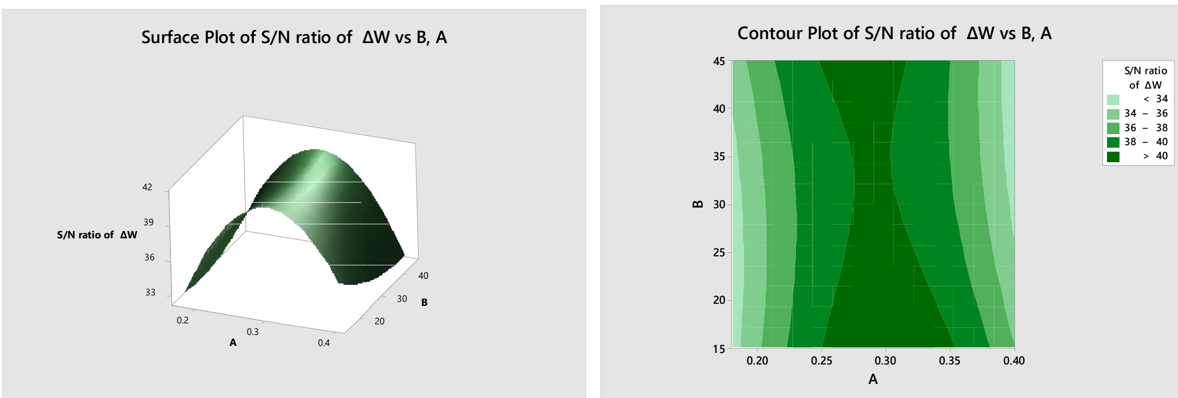


(a) (b)

Figure 4.11 (a-b) 3D Surface and contour plots for S/N ratio of ΔW against Infill(B) and Layer height(A)

Figure 4.12 (a-b) shows 3D surface and contour plot of the interaction analysis between infill and layer height for mean ΔT. From this plot, it is clearly show that the lower ΔT is observed at layer height between 0.35 mm and 0.40 mm and at Infill between 15% and 20 %. At the middle of layer height and higher Infill value, the ΔT was higher. Therefore, optimum means ΔL can be obtained at the lower layer height and infill rate value.

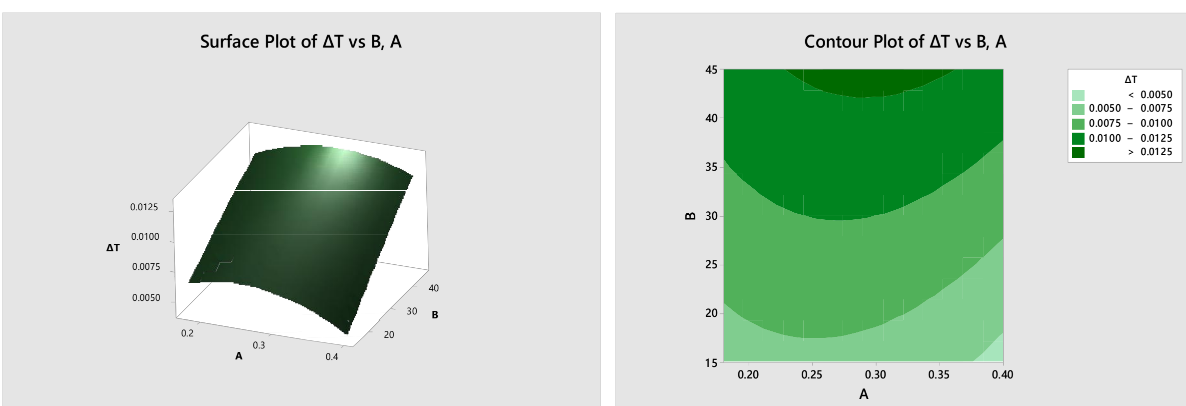


(a) (b)

Figure 4.12 (a-b) 3D Surface and contour plots for mean ΔT against Infill(B) and Layer height(A)

Figure 4.13 (a-b) shows 3D surface and contour plot of the interaction analysis between infill and layer height for S/N ratio of ΔT. From this plot, it is clearly show that the higher S/N ratio of ΔT is observed at layer height between 0.40 mm and 0.45 mm and at Infill between 15 % and 20 %. At all value of layer height and higher Infill value, the S/N ratio of ΔT is low. Therefore, it can be conclude that layer height has insignificant effect on S/N ratio of ΔT.

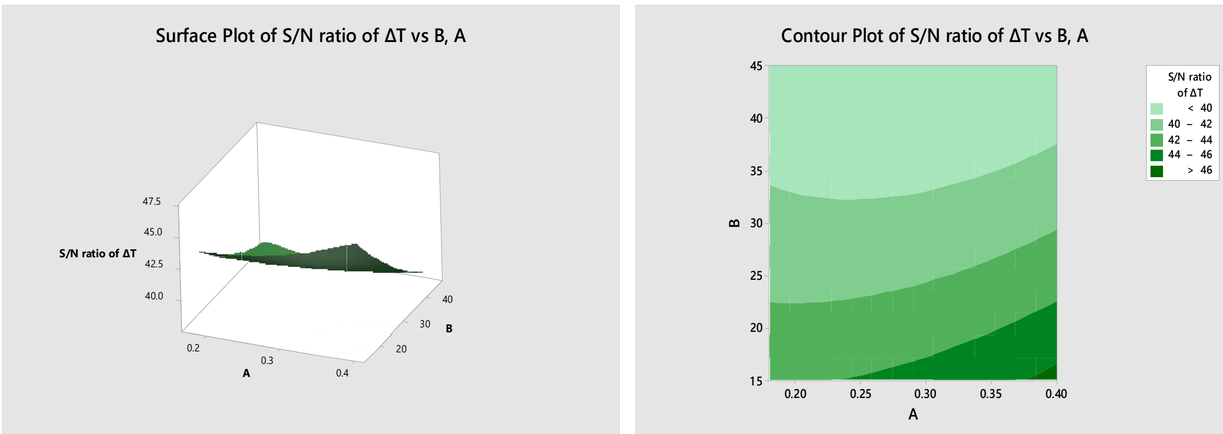


(a) (b)

Figure 4.13 (a-b) 3D Surface and contour plots for S/N ratio of ΔT against Infill(B) and Layer(A) height

Figure 4.14 (a-b) shows 3D surface and contour plot of the interaction analysis between infill and layer height for mean ΔL. From this plot, it is clearly show that the lower ΔL is observed at layer height between 0.35 mm and 0.40 mm and at Infill between 15% and 20 %. At the layer height higher and middle of Infill value, the ΔL was higher. Therefore, optimum means percentage ΔL can be obtained at the lower layer height and infill rate value.

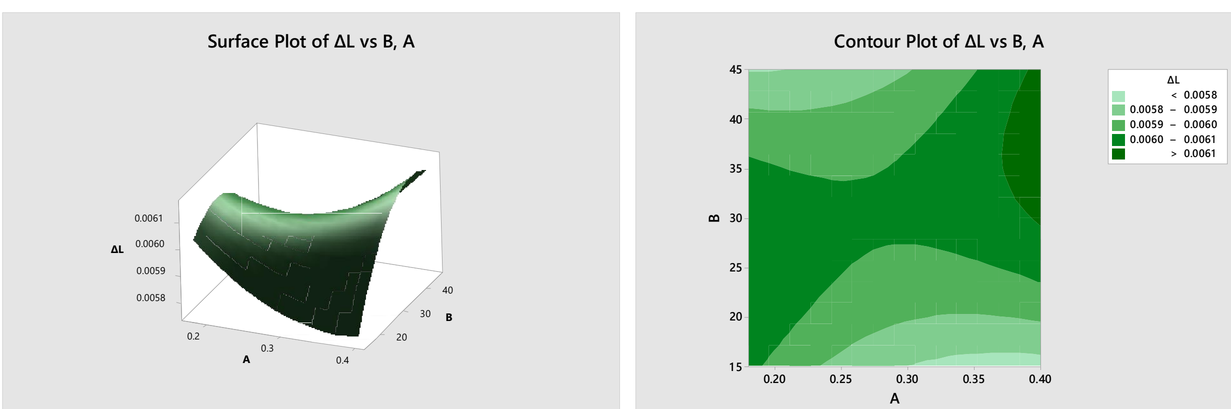


(a) (b)

Figure 4.14 (a-b) 3D Surface and contour plots for mean ΔL against Infill and Layer height

Figure 4.15 (a-b) shows 3D surface and contour plot of the interaction analysis between infill and layer height for S/N ratio of ΔL. From this plot, it is clearly show that the higher S/N ratio of ΔL is observed at layer height between 0.40 mm and 0.45 mm and at Infill between 15 % and 20 %. At higher layer height and Infill value, the S/N ratio of ΔT is low.

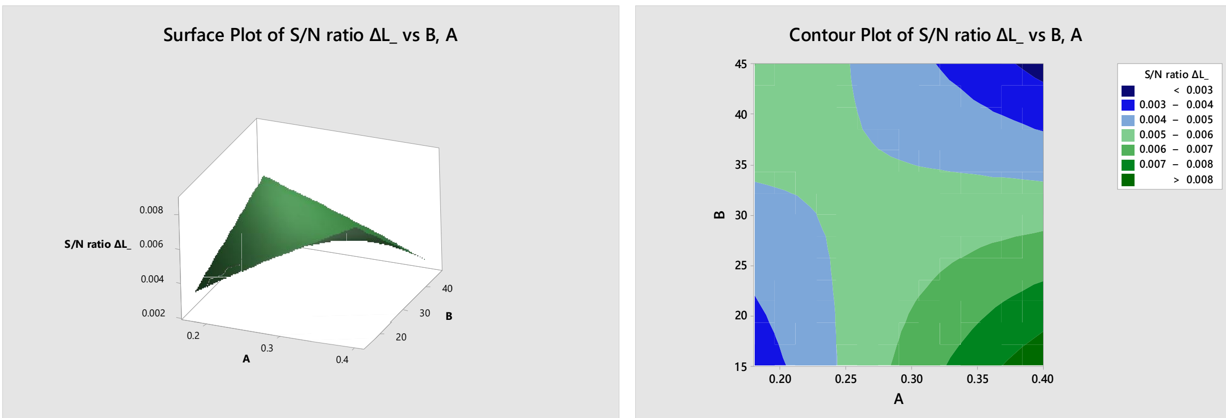


(a) (b)

Figure 4.15 (a-b) 3D Surface and contour plots for S/N ratio of **%** ΔT against Infill and Layer height

After complete analysis of 3D surface and contour plot of the interaction, we can predict that at layer height between 0.30 mm to 40mm and infill rate (15% to 20%) could yield minimum deviation of dimensional accuracy for width, length, and thickness. It can be summarize that to obtain a good dimensional accuracy, it is recommended to use a high layer height and low infill rate.

## 4.7 Response optimization for Dimensional accuracy

Optimization using Taguchi methods have three condition; smaller is better, nominal is better and large is better. In this condition of dimensional accuracy (ΔW, ΔT and ΔL), the smaller are the optimal condition. Process parameters settings with the highest S/N ratio always yield the optimum quality with minimum variance. Based on the S/N analysis, the optimal process parameters for dimensional accuracy (ΔW, ΔT and ΔL) are the layer height at level – 2, the Infill rate at level – 1, Build speed at level – 1 and the build temperature at level – 1. Table 4.14 – 4.16 shows Optimum setting parameters for dimensional accuracy (ΔW, ΔT, and ΔL).

Table 4.14 Optimum response tables for Relative change in dimension of width (ΔW)

| Factors | Level | Optimized Value | |
|---|---|---|---|
| Layer height | 2 | 0.290 mm | Optimum ΔW = **0.0048** |
| Infill rate | 1 | 15 % | At maximum value of |
| Build speed | 1 | 60 mm/min | |
| Build temperature | 1 | 220 ºC | **S/N ratio = 46.3752** |

Table 4.15 Optimum response tables for dimensional accuracy (**%** ΔT)

| Factors | Level | Optimized Value | |
|---|---|---|---|
| Layer height | 2 | 0.290 mm | Optimum % ΔT = **0.0044** |
| Infill rate | 1 | 15 % | At maximum value of |
| Build speed | 1 | 60 mm/sec | |
| Build temperature | 1 | 220 ºC | **S/N ratio = 47.1309** |

Table 4.16 Optimum response tables for dimensional accuracy (**%** ΔL)

| Factors | Level | Optimized Value | |
|---|---|---|---|
| Layer height | 2 | 0.290 mm | Optimum % ΔL = **0.0056** |
| Infill rate | 1 | 15 % | At maximum value of |
| Build speed | 1 | 60 mm/sec | |
| Build temperature | 1 | 220 ºC | **S/N ratio = 45.0362** |

## 4.8 Validation of optimum setting

Experiments were conduct to ensure performance on optimum condition and the results were tabulate in Table – 4.17. From the results, it observed that optimized condition gives good dimensional accuracy (ΔW, ΔT and ΔL). To confirm the optimized value, experiment was conduct with same set of parameters and the dimensional accuracy (ΔW, ΔT and ΔL) observed. The initial reading of dimensional accuracy (ΔW, ΔT and ΔL) was ΔW = 0.0048, ΔT=0.0044 and ΔL=0.0056. After setting the parameters to the optimized values, the response characteristic has been changed to ΔW = 0.00492, ΔT=0.00462and ΔL=0.00584.

Table 4.17 Results of the confirmation experiments for optimized condition dimensional accuracy (ΔW, ΔT and ΔL)

| Optimal level | Response obtained | | |
|---|---|---|---|
| | Initial reading (predicted result) | After reading (Exp. result) | |
| **% ΔW** | 0.0048 mm | 0.00492 | Error % = 2.5% $= \frac{(\text{Exp.Result} - \text{predicted result}) * 100}{Experimental\ result}$ |
| **% ΔT** | 0.0044 mm | 0.00462 | Error % = 4.76% $= \frac{(\text{Exp.Result} - \text{predicted result}) * 100}{Experimental\ result}$ |
| **% ΔL** | 0.0056 mm | 0.00584 | Error % = 4.11% $= \frac{(\text{Exp.Result} - \text{predicted result}) * 100}{Experimental\ result}$ |

# Chapter 5
# Result and Discussion of Surface roughness (Ra)

## 5.1 Introduction

In this section results of surface roughness are analyzed and optimized using Taguchi method. The effects of each process parameters like; layer height, infill, build speed, and build temperature on surface roughness of produced parts is analyzed using Analysis of Variance, Main effect plots, Interaction plots, 3D Surface plots and Contour plots. Surface roughness of each fabricated part is measured at five different places on the top and bottom surfaces and the average value is used for analysis purpose. the unit of measurement is **µm**. Analysis of Variance, Main effect plots, Interaction plots, 3D Surface plots and Contour plots for surface roughness are constructed with the help of Minitab V18.1 software, to analyze the relationship between each process parameters. Optimum setting was determined using S/N ratio.

## 5.2 Result of surface roughness

The mean surface roughness (Ra) and S/N ratios for each of nine experimental trials are given in Table 5.1. S/N ration was calculated using MINITAB V18.1 trial software. Figure 5.1 shows the distribution of the resulting data appears to be normal but cyclic in nature from minimum to maximum and then minimum.

Table 5.1 Experimental results for Mean surface roughness and S/N ratio

| Run | Layer height mm | Infill % | Build speed mm/min | Build temperature ºC | Mean Ra µm | SNRA |
|---|---|---|---|---|---|---|
| 1 | 0.180 | 15 | 60 | 220 | 16.862 | -24.5382 |
| 2 | 0.180 | 30 | 120 | 230 | 17.908 | -25.0609 |
| 3 | 0.180 | 45 | 180 | 240 | 11.703 | -21.3659 |
| 4 | 0.290 | 15 | 60 | 220 | 7.779 | -17.8185 |
| 5 | 0.290 | 30 | 120 | 230 | 9.074 | -19.1560 |
| 6 | 0.290 | 45 | 180 | 240 | 8.302 | -18.3837 |
| 7 | 0.40 | 15 | 60 | 220 | 12.826 | -22.1618 |
| 8 | 0.40 | 30 | 120 | 230 | 22.798 | -27.1579 |
| 9 | 0.40 | 45 | 180 | 240 | 21.440 | -26.6245 |

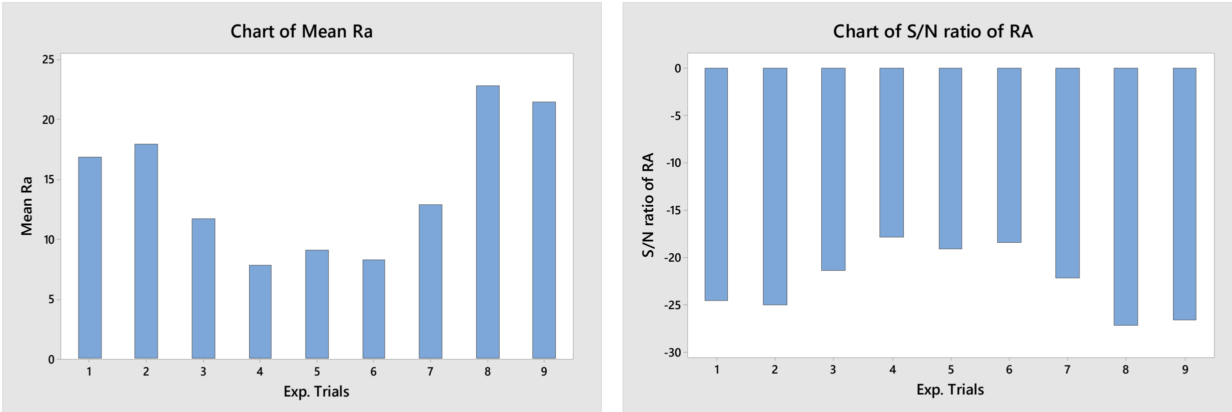


(a) (b)

Figure 5.1 Bar chart plots for mean and S/N ratio of Ra.

## 5.3 Taguchi analysis for surface roughness (Ra)

Table 5.2 and 5.3 shows rank of various factors in terms their relative significance on surface roughness (Ra). It clearly shows that surface roughness (Ra) is most significantly affected by layer height and Build temperature has insignificant effect. Table 5.2 shows response table for mean surface roughness and Table 5.3 shows response table for S/N ratio of surface roughness.

Table 5.2 Response table for mean Ra

| Levels | Layer height mm | Infill % | Build speed mm/min | Build temperature ºC |
|---|---|---|---|---|
| 1 | -23.66 | -21.51 | -23.36 | -23.44 |
| 2 | -18.45 | -23.79 | -23.17 | -21.87 |
| 3 | -25.31 | -22.12 | -20.89 | -22.11 |
| Delta | 6.86 | 2.29 | 2.47 | 1.57 |
| Rank | 1 | 3 | 2 | 4 |

Table 5.3 Response table for S/N ratio of Ra

| Level | Layer height mm | Infill % | Build speed mm/min | Build temperature ºC |
|---|---|---|---|---|
| 1 | 23.66 | 21.51 | 23.36 | 23.44 |
| 2 | 18.45 | 23.79 | 23.17 | 21.87 |
| 3 | 25.31 | 22.12 | 20.89 | 22.11 |
| Delta | 6.86 | 2.29 | 2.47 | 1.57 |
| Rank | 1 | 3 | 2 | 4 |

## 5.4 Analysis of variance for surface roughness (Ra)

Table 5.4 and Table 5.5 shows results of analysis of variance (ANOVA) for the mean and S/N ratio of surface roughness (Ra) at 95% confidence interval respectively. The principle of the F-test and P- test is that the larger F value and smaller P value for a particular parameter, the greater the effect on the performance characteristic due to the change in that process parameter. If the P-value is less than 0.05(i.e., $\alpha = 0.05$, or 95% confidence level) then the given parameter is significant. ANOVA table for mean and S/N ratio of surface roughness (Ra) shows that P – value 0.027 and 0.021 respectively, which is less than 0.05 for layer height, this shows that layer height is dominant parameter.

Table 5.4 Analysis of Variance for means surface roughness (Ra)

| Source | DF | Adj SS | Adj MS | F-Value | P-Value |
|---|---|---|---|---|---|
| Layer height | 2 | 176.09 | 88.05 | 6.39 | 0.027 |
| Infill | 2 | 26.32 | 13.16 | 0.96 | 0.458 |
| Build temperature | 2 | 32.58 | 17.92 | 1.31 | 0.401 |
| Build speed | 2 | 14.26 | 9.43 | 0.07 | 0.584 |
| Error | 4 | 8.25 | 3.77 | | |
| Total | 12 | 257.50 | | | |

Table 5.5 Analysis of Variance for S/N ratio of surface roughness (Ra)

| Source | DF | Adj SS | Adj MS | F-Value | P-Value |
|---|---|---|---|---|---|
| Layer height | 2 | 76.905 | 38.453 | 9.88 | 0.021 |
| Infill | 2 | 8.384 | 4.192 | 1.08 | 0.402 |
| Build temperature | 2 | 9.257 | 5.213 | 1.42 | 0.392 |
| Build speed | 2 | 5.286 | 2.587 | 0.04 | 0.681 |
| Error | 4 | 1.025 | 1.892 | | |
| Total | 12 | 100.857 | | | |

## 5.5 Main effect and interaction plot for mean and S/N ratio of surface roughness

Figure 5.2 show main effect plots for mean and S/N ratio of $\Delta W$. main effect plot for mean Ra clearly shows that Ra decreases with increasing layer height until 0.29 mm after this point it start to increase for further increase in layerhight. In other case, increasing infill rate will increase Ra but after 30 %, it starts to decrease. Ra decrease with increasing build speed. Ra decrease with increasing build temperature but after 230 ºC, it starts to increase slightly. From main effect plot for S/N ratio of Ra, it is clearly indicates that the S/N ratio of Ra increases with increasing layer height until 0.29 mm after this point it start to decrease. In other case, increasing infill rate will decrease S/N ratio of Ra but after 30 %, it starts to increase. S/N ratio of Ra increases with increasing build speed. S/N ratio of Ra increase with increasing builds temperature but after 230 ºC, it starts to decrease slightly. Figure 5.3 shows the interaction between process parameters on the Ra.

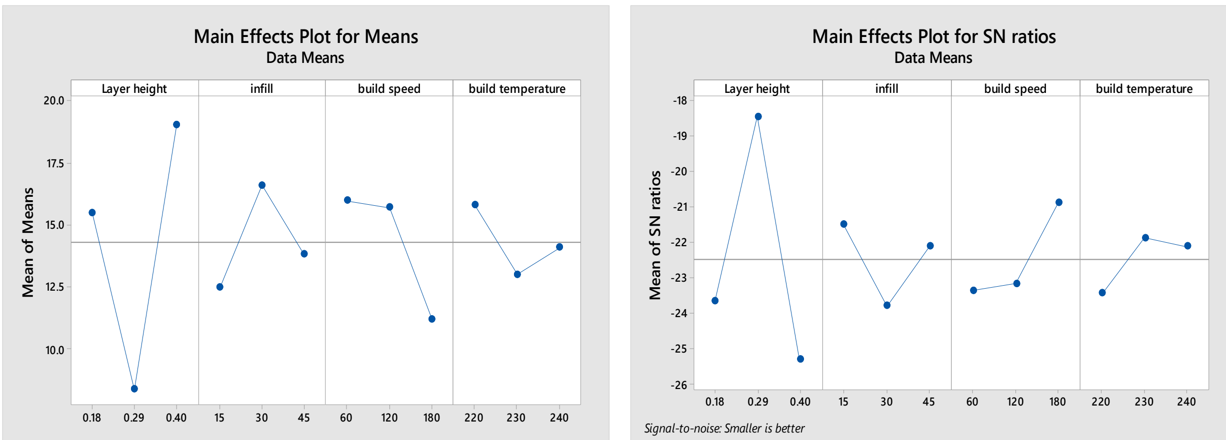


(a) (b)

Figure 5.2 Main effect plot for mean and S/N ratio of Ra

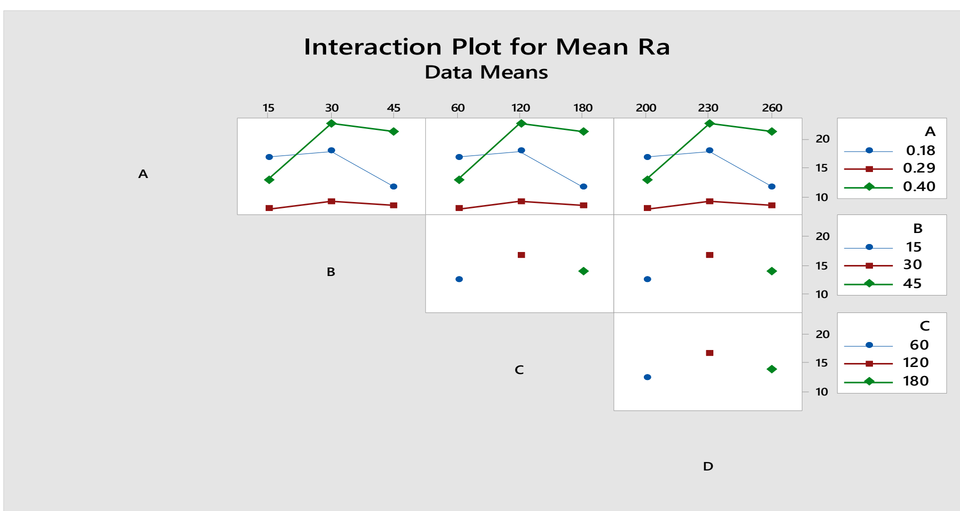


Figure 5.3 Interaction plot for Ra means with all process parameters

## 5.6 3D Surface and Contour plot for surface roughness (Ra)

3D surface and contour graphs are, constructed for surface roughness against Layer height, Infill, Build speed and Build temperature, to analysis the relationship between each process parameters.

Figure 5.4 (a-b) shows 3D surface and contour plot of the interaction analysis between infill(B) and layer height(A) for mean surface roughness. From this plot, it is clearly shown that the lower surface roughness is observed at layer height between 0.25 mm and 0.35 mm, and at Infill between 15 % and 20 %. At higher layer height and at the middle infill, the surface roughness was higher. Therefore, optimum means surface roughness can be obtained at the middle of layer height and lower infill rate value. Here the surface plot is **monotonic** since Mean Ra is strictly increasing after the interval of optimal points,layer hight [0.25,0.35] mm and infill [15,20] %.

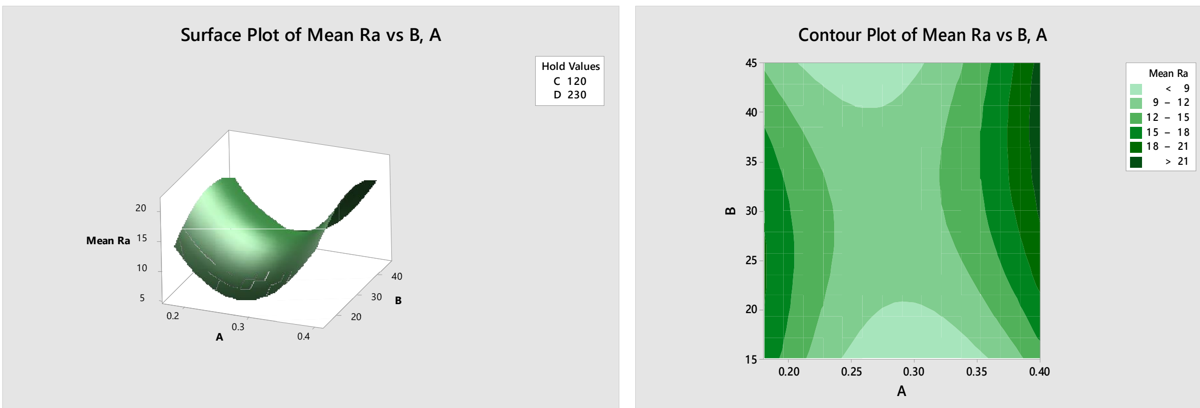


(a) (b)

Figure 5.4 (a-b): 3D Surface and contour plots of surface roughness against Infill(B) and Layer height(A).

Figure 5.5 (a-b) shows 3D surface and contour plot of the interaction analysis between build speed(C) and layer height(A) for mean surface roughness. From this plot, it is clearly shown that the lower surface roughness is observe at layer height between 0.25 mm and 0.35 mm, and at build speed between 160 mm/sec and 180 mm/sec. At higher layer height and lower infill, the surface roughness was higher. Therefore, optimum means surface roughness can be obtained at the middle of layer height and higher build speed value. Here the surface plot is **monotonic** since Mean Ra is strictly increasing after the interval of optimum points layer hight [0.25,0.35] mm and build speed [15,20] mm/sec.

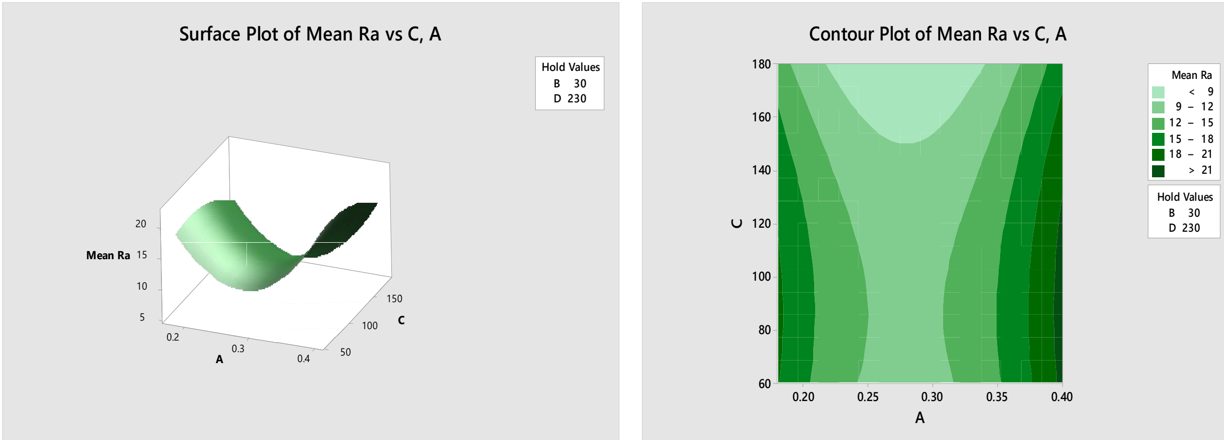


(a) (b)

Figure 5.5 (a-b): 3D Surface and contour plots of surface roughness against Build speed(C) and Layer height(A).

Figure 5.6 (a-b) shows 3D surface and contour plot of the interaction analysis between build temperature (D) and layer height(A) for mean surface roughness. From this plot, it is clearly shown that the lower surface roughness is observed at layer height between 0.25 mm and 0.35 mm, and at build temperature between 226 ºC and 235 ºC. At the higher layer height and lower build temperature, the surface roughness was higher. Therefore, optimum means surface roughness can be obtained at the middle of layer height and build temperature. 3D surface plot have a convex shape because all set of points lying above the optimum points.

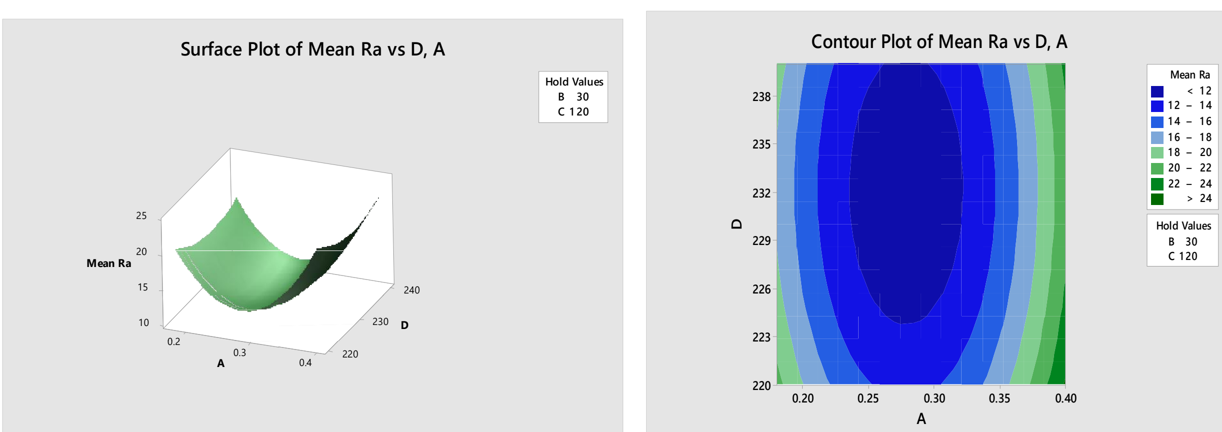


(a) (b)

Figure 5.6 (a-b): 3D Surface and contour plots of surface roughness against Build temperature (D) and Layer height (A)

Figure 5.7 (a-b) shows 3D surface and contour plot of the interaction analysis between Build speed(C) and Infill (B) for mean surface roughness. From this plot, it is clearly shown that the lower surface roughness is observed at infill between 15 % and 20 %, and at build speed between 160 mm/sec and 180 mm/sec. At the middle of infill and lower build speed, the surface roughness was higher. Therefore, optimum means surface roughness can be obtained at the lower infill and higher build speed. Here the surface plot have a **concave** shape because all set of points lying below the optimum points.

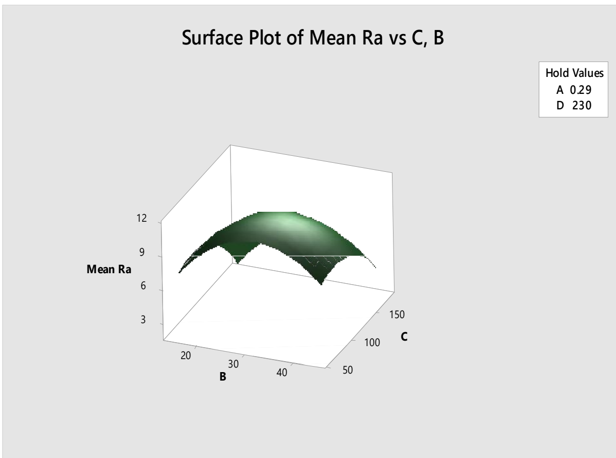


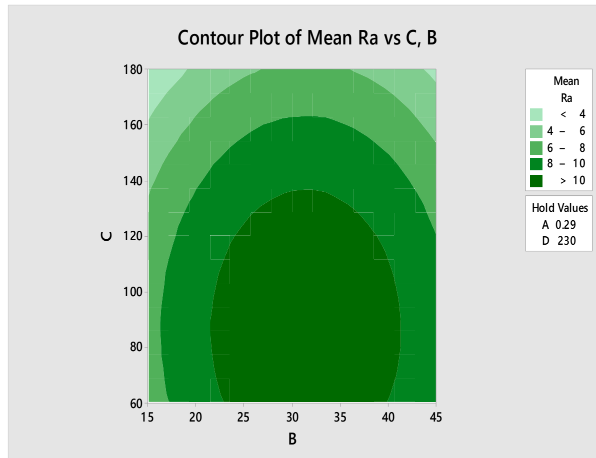


(a) (b)

Figure 5.7 (a-b): 3D Surface and contour plots of surface roughness against Build speed(C) and Infill (B)

Figure 5.8 (a-b) shows 3D surface and contour plot of the interaction analysis between Build temperature and Infill for mean surface roughness. From this plot, it is clearly shows that the lower surface roughness is observed at infill between 15 % and 20 %, and at build temperature between 226 ºC and 235 ºC. At the middle of infill and lower temperature, the surface roughness was higher. Therefore, optimum means surface roughness can be obtained at lower infill and middle build temperature value. Here the surface plot is monotonic since Ra is decreasing after the interval of optimum points infill [15,20] % and build temperature [226,235] ºC.

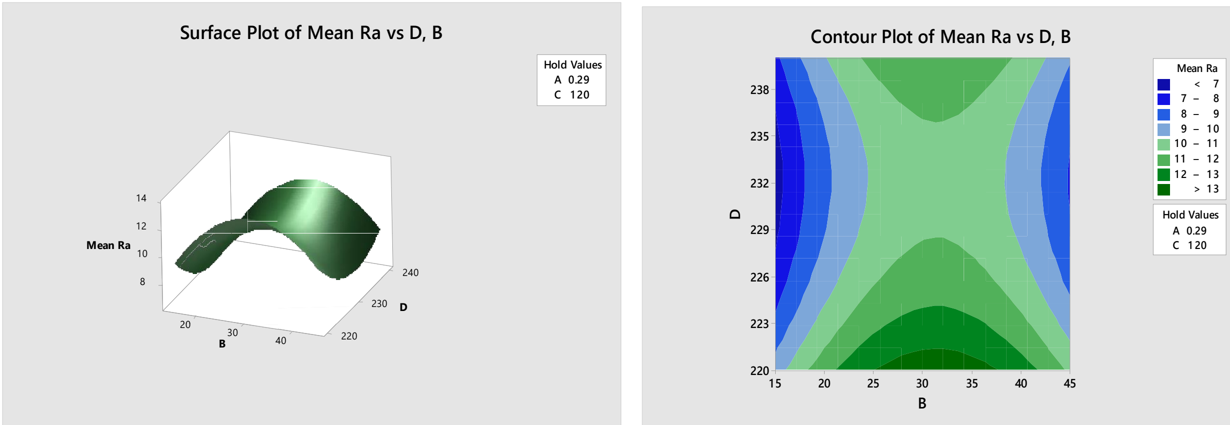


(a) (b)

Figure 5.8 (a-b): 3D Surface and contour plots of surface roughness against Build temperature (D) and Infill(B)

Figure 5.9 (a-b) shows 3D surface and contour plot of the interaction analysis between Build temperature and Build Speed for mean surface roughness. From this plot, it is clearly shows that the lower surface roughness is observed at build speed between 160 mm/sec and 180 mm/sec, and at build temperature between 226 ºC and 235 ºC. At lower build speed and build temperature, the surface roughness was higher. Therefore, optimum means surface roughness can be obtained at higher build speed and middle build temperature value. Here the surface plot is **monotonic** since Mean Ra is decreasing after the intervals of optimal points,build speed [160,180] mm/sec and build temperature [226,235] ºC.

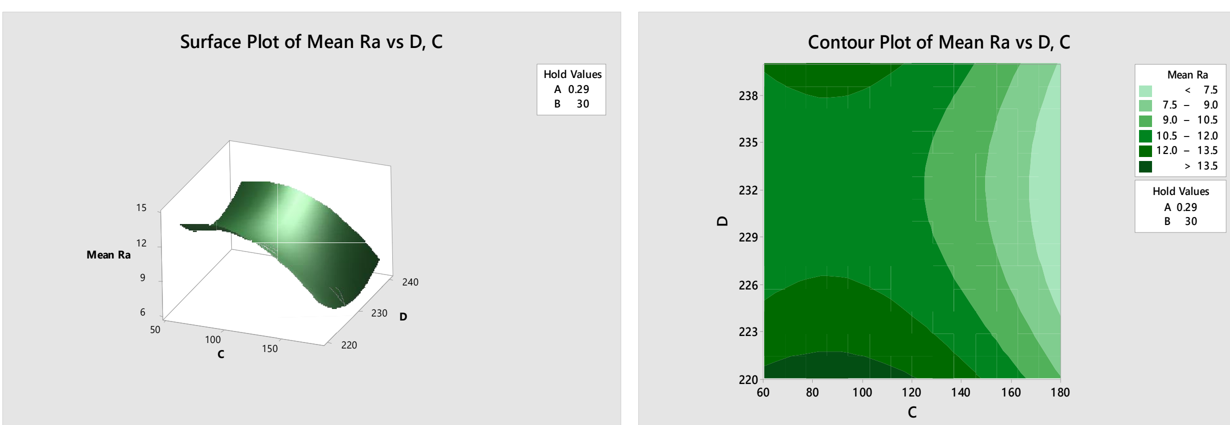


(a) (b)

Figure 5.14 (a-b): 3D Surface and contour plots of surface roughness against Build temperature(C) and Build Speed(D)

After complete analysis of 3D surface and contour plot of the interaction, we can predict that at Layer height between 0.25 mm and 0.35 mm, Infill between 15 % and 20 %, Build speed between 160 mm/sec and 180mm/sec and Build temperature 226 ºC to 235 ºC could yield best surface roughness (lower surface roughness). It can be summarized that to obtain a good surface roughness, it is recommended to use at middle value of layer height, low infill, high build speed and at middle of build temperature.

### 5.7 Response optimization of Surface roughness (Ra)

Optimization using Taguchi methods have three condition; smaller is better, nominal is better and large is better. In this condition of surface roughness (Ra), the smaller are the optimal condition. The S/N ratio is used to a measure of performance to develop products and processes in sensitive to noise factors. Process parameters settings with the highest S/N ratio always yield the optimum quality with minimum variance. Based on the S/N analysis, the optimal process parameters for surface roughness (Ra) are the layer height at level – 2, the Infill rate at level – 1, Build speed at level – 1 and the build temperature at level – 1. Table 5.6 shows Optimum setting parameters for surface roughness (Ra).

Table 5.6 Optimum response tables for surface roughness (Ra).

| Factors | Code | Level | Optimize value | |
|---|---|---|---|---|
| **Layer height** | A | 2 | 0.29mm | **Optimum Value Ra =7.779 µm At maximum value of S/N ratio = - 17.8185** |
| **Infill** | B | 1 | 15 | |
| **Build speed** | C | 1 | 60 mm/min | |
| **Build temperature** | D | 1 | 220 ºc | |

### 5.7 Validation of optimum setting

Experiments were conduct to ensure performance on optimum condition and the result were tabulate in Table – 5.7. From the results it is observed that optimized condition gives good surface roughness. To confirm the optimized value, an experiment was conducted with same set of parameters and the surface roughness was observed. The initial reading of surface roughness was Ra = 7.779 µm. After setting the parameters to the optimized values, the response characteristic has been changed to Ra = 7.891 µm.

Table 5.7 Results of the confirmation experiments for optimized condition of mean Ra.

| **Optimal level** | **Response obtained** | | |
|---|---|---|---|
| | **Initial reading** (predicted result) | **After reading** (Exp. result) | **Error % = 1.419 %** $= \frac{(\text{Exp.Result} - \text{predicted result}) * 100}{\textit{Experimental result}}$ |
| **Mean Surface roughness value** | 7.779 μm | 7.891 μm | |

# Chapter 6
# Result and Discussion of Mechanical property (Tensile strength)

## 6.1 Introduction

In this section result of Tensile strength are analyzed and optimized using Taguchi methods. Effect of process parameters like; layer height, infill, build speed, and build temperature on Tensile strength of produced parts using Flash forge FDM machine are optimized using Taguchi method. Tensile strength of each fabricated parts are measured longitudinally using Testmetric, the unit of measure is MPa. Variance of analysis, Main effect plots, Interaction plots, 3D Surface plots and Contour plots for Tensile strength are constructing with the help of Minitab V18.1 software, to analysis the relationship between each process parameters. Optimum setting was determined using S/N ratio

## 6.2 Result of Tensile strength

The tensile tests were carried out using a testometric material testing machine 350 KN maximum capacity, The cross head speed of this machine is 1mm/min and the test stops once the specimens broken. The material used for specimen preparation is ABS with a nominal thickness of 5 mm, width 12 mm and the tensile strength is calculated by dividing maximum load(load at break) with original cross sectional area(original width × original thickness). The results of Tensile strength (UTS) for each of 9 experiments are given in Table 6.1. Figure 6.1 bar chart plots for mean and S/N ratio of Tensile strength (UTS), shows Distribution of Tensile strength (UTS) for each experimental trial. S/N ration was calculated using MINITAB V18 trial software.

Table 6.1 Experimental results for Tensile strength (UTS) and S/N ratio

| Run | Layer height mm | Infill % | Build speed mm/min | Build temperature °C | UTS MPa | S/N ratio |
|---|---|---|---|---|---|---|
| 1 | 0.180 | 15 | 60 | 220 | 21.945 | 26.8267 |
| 2 | 0.180 | 30 | 120 | 230 | 35.934 | 31.1101 |
| 3 | 0.180 | 45 | 180 | 240 | 39.094 | 31.8422 |
| 4 | 0.290 | 15 | 60 | 220 | 30.383 | 29.6526 |
| 5 | 0.290 | 30 | 120 | 230 | 38.952 | 31.8106 |
| 6 | 0.290 | 45 | 180 | 240 | 23.964 | 27.5912 |
| 7 | 0.40 | 15 | 60 | 220 | 36.715 | 31.2969 |
| 8 | 0.40 | 30 | 120 | 230 | 34.946 | 30.8679 |
| 9 | 0.40 | 45 | 180 | 240 | 28.743 | 29.1706 |

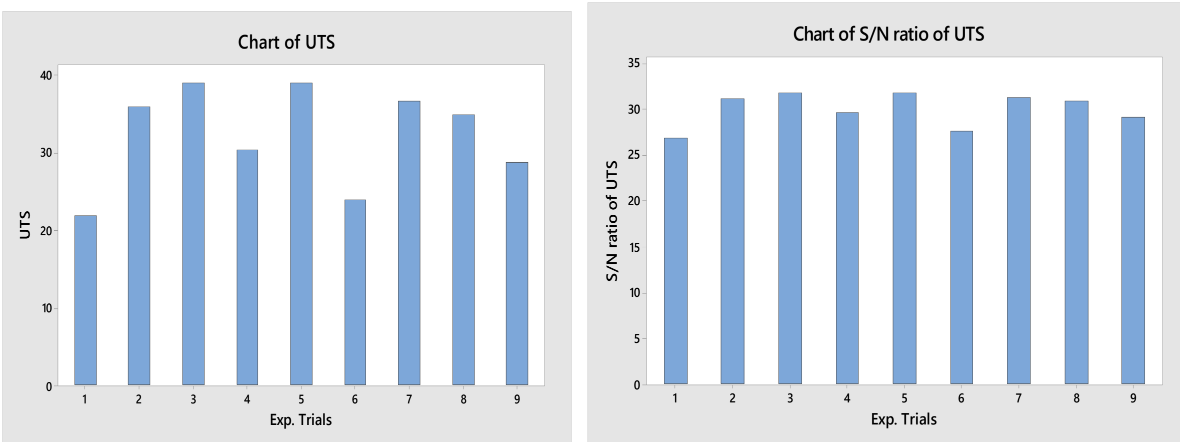


Figure 6.1 Bar chart plots for mean and S/N ratio of Tensile strength (UTS)

## 6.3 Taguchi analysis for Tensile strength (UTS)

Results of Tensile strength (UTS) were analyzed using Taguchi analysis. Table 6.2 and 6.3 shows rank of various factors in terms their relative significance for Tensile strength (UTS). It clearly shows that Tensile strength (UTS) has most significantly affected by Infill and layer height has insignificant effect. Table 6.2 shows response table for Tensile strength (UTS) and Table 6.3 shows response table for S/N ratio of Tensile strength (UTS).

Table 6.2 Response table for Tensile strength (UTS)

| Levels | Layer height mm | Infill % | Build speed mm/min | Build temperature ºC |
|---|---|---|---|---|
| **1** | 32.32 | 29.68 | 26.95 | 29.88 |
| **2** | 31.10 | 36.61 | 31.69 | 32.20 |
| **3** | 33.47 | 30.60 | 38.25 | 34.81 |
| **Delta** | 2.37 | 6.93 | 11.30 | 4.93 |
| **Rank** | 4 | 1 | 2 | 3 |

Table 6.3 Response table for S/N ratio of Tensile strength (UTS)

| Levels | Layer height mm | Infill % | Build speed mm/min | Build temperature ºC |
|---|---|---|---|---|
| **1** | 29.93 | 29.26 | 28.43 | 29.27 |
| **2** | 29.68 | 31.26 | 29.98 | 30.00 |
| **3** | 30.45 | 29.53 | 31.65 | 30.79 |
| **Delta** | 0.76 | 2.00 | 3.22 | 1.52 |
| **Rank** | 4 | 1 | 2 | 3 |

## 6.4 Analysis of variance for Tensile strength (UTS)

The results for Tensile strength (UTS) were analyzed using ANOVA for identifying the significant factors affecting the performance measures. In Table 6.4 and Table 6.5 shows result of analysis of variance (ANOVA) for the mean and S/N ratio of Tensile strength (UTS) at 95% confidence interval is given respectively. For significance check F – value and P – value given in ANOVA table is used. The principle of the F-test and P- test is that the larger F value and smaller value for a particular parameter, the greater the effect on the performance characteristic due to the change in that process parameter. If the P- value less than 0.0500 (i.e., α = 0.05, or 95% confidence level) indicate process parameters term are significant. ANOVA table for mean and S/N ratio for Tensile strength (UTS) shows that P – value 0.048 and 0.049 respectively that is less than 0.05 for infill density, this shows that infill density is the significant factor that affects the mean and S/N ratio of Tensile strength (UTS).

Table 6.4 Analysis of Variance for means Tensile strength (UTS)

| Source | DF | Adj SS | Adj MS | F-Value | P-Value |
|---|---|---|---|---|---|
| **Layer height** | 2 | 8.417 | 4.208 | 0.07 | 0.931 |
| **Infill** | 2 | 84.990 | 42.495 | 1.74 | 0.048 |
| **Build speed** | 2 | 43.31 | 21.654 | 1.13 | 0.329 |
| **Build temperature** | 2 | 11.78 | 5.892 | 0.05 | 0.741 |
| **Error** | 4 | 2.599 | 0.5199 | | |
| **Total** | 12 | 151.096 | | | |

Table 6.5 Analysis of Variance for S/N Tensile strength (UTS)

| Source | DF | Adj SS | Adj MS | F-Value | P-Value |
|---|---|---|---|---|---|
| **Layer height** | 2 | 0.9056 | 0.4528 | 0.10 | 0.911 |
| **Infill** | 2 | 23.0794 | 3.5397 | 1.87 | 0.049 |
| **Build speed** | 2 | 11.283 | 5.642 | 1.45 | 0.329 |
| **Build temperature** | 2 | 4.284 | 2.142 | 0.30 | 0.851 |
| **Error** | 4 | 1.0321 | 4.7580 | | |
| **Total** | 12 | 40.5851 | | | |

## 6.5 Main effect and interaction plot for mean and S/N ratio of Tensile strength(UTS)

Figure 6.2 shows main effect plot for mean and S/N ratio of Tensile strength (UTS). It is clearly shows that , Tensile strength (UTS) decreases with increasing layer height until 0.29 mm but after this point, it starts to increase. In other case, increasing infill rate will increase Tensile strength (UTS) but after 30 %, it starts to decrease. Tensile strength (UTS) increasing with increasing builds speed. In other case, Tensile strength (UTS) increasing with increasing Build temperature. Figure 6.3 shows the interaction between process parameters on the Tensile strength (UTS).

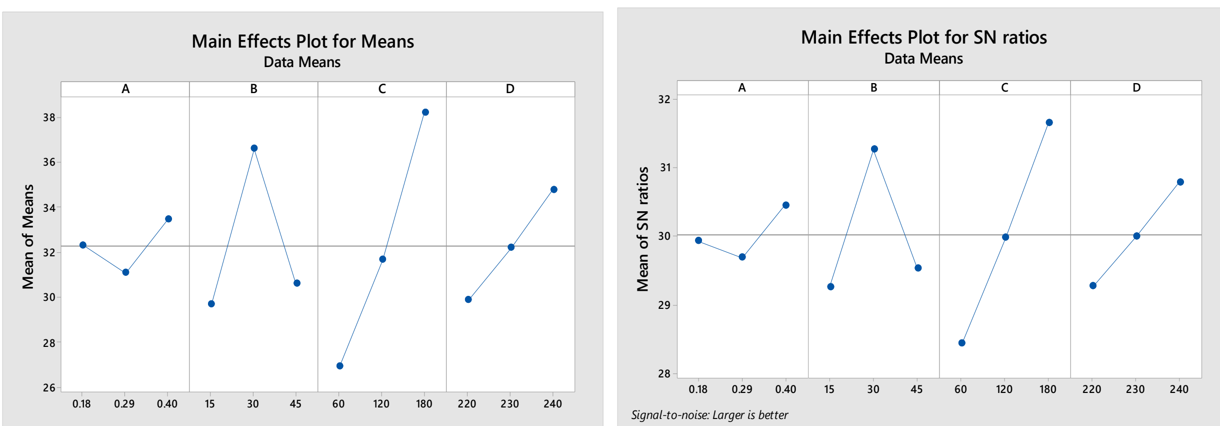


(a) (b)

Figure 6.2 Main effect plot for mean and S/N ratio of Tensile strength (UTS)

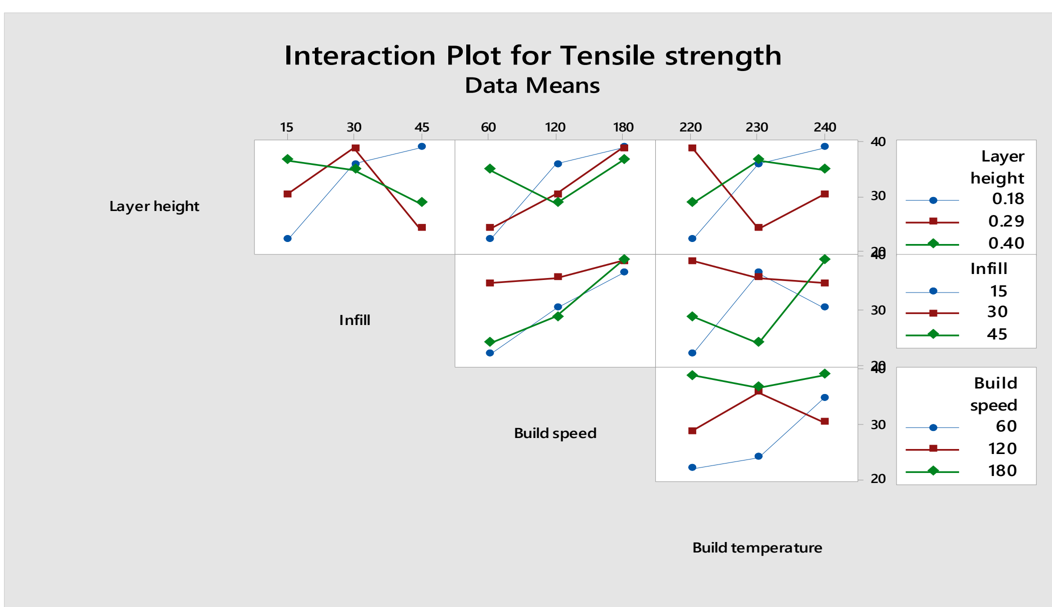


Figure 6.3 Interaction plot for Ra means with all process parameters

## 6.6 3D Surface and Contour plot for Tensile strength

3D surface and contour graphs are, plot for Tensile strength (UTS) against Layer height, Infill, Build speed and Build temperature, creating to analysis the relationship between each process parameters. Figure 6.4 (a-b) shows 3D surface and contour plot of the interaction analysis between infill and layer height for mean Tensile strength. From this plot, it is clearly show that the higher Tensile strength is observed at layer height between 0.20 mm and 0.25 mm, and at Infill between 35 % and 40 %. At lower layer height and Infill, the Tensile strength was lower. Therefore, optimum means Tensile strength can be obtained at the lower layer height and higher infill rate value.

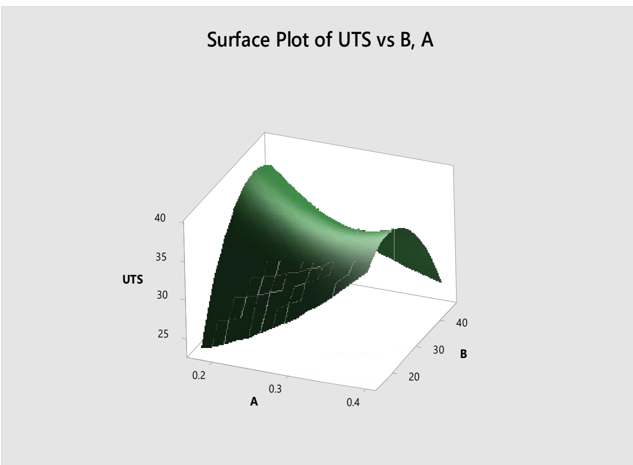


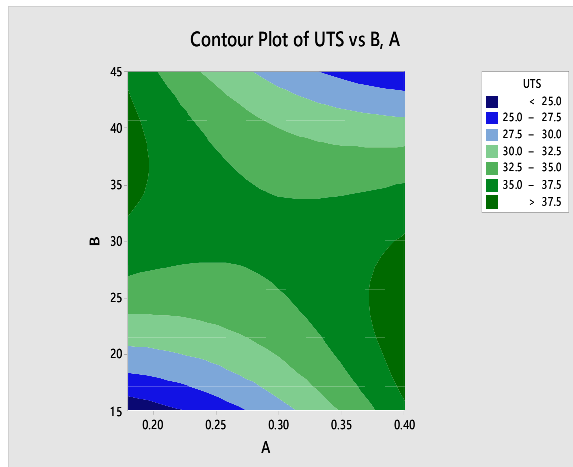


(a) (b)

Figure 6.4 (a-b): 3D Surface and contour plots of Tensile strength against Infill and Layer height

Figure 6.5 (a-b) shows 3D surface and contour plot of the interaction analysis between infill and layer height for S/N ratio of Tensile strength. From this plot, it is clearly show that the higher S/N ratio of Tensile strength is observed at layer height between 0.20 mm and 0.25 mm, and at Infill between 35 % and 40 %. At lower layer height and Infill, the S/N ratio of Tensile strength was lower. Therefore, optimum means Tensile strength can be obtained at the lower layer height and higher infill rate value.

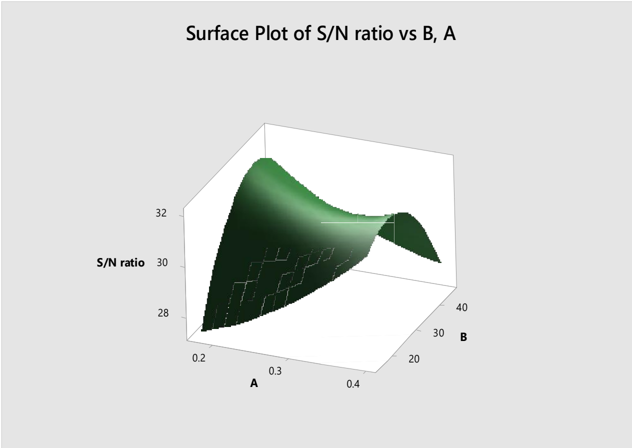


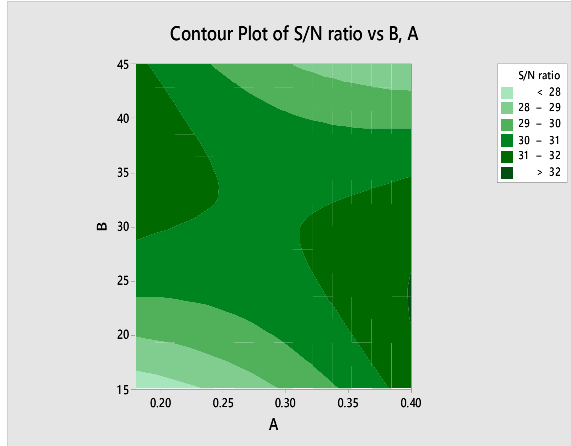


(a) (b)

Figure 6.5 (a-b): 3D Surface and contour plots for S/N ratio of Tensile strength against Infill and Layer height

After complete analysis of 3D surface and contour plot of the interaction, we can predict that at Layer height between 0.20mm to 0.25 mm and infill between 35 % to 40% could yield best Tensile strength (maximum tensile strength). It can be summarized that to obtain a higher tensile strength, it is recommended to use a low Layer height between and high infill.

### 6.7 Response optimization Tensile strength

Optimization using Taguchi methods have three condition; smaller is better, nominal is better and large is better. In this condition of Tensile strength (UTS), the larger are the optimal condition. The S/N ratio is used to a measure of performance to develop products and processes in sensitive to noise factors. Process parameters settings with the highest S/N ratio always yield the optimum quality with minimum variance. Based on the S/N analysis, the optimal process parameters for Tensile strength (UTS) are the layer height at level – 1, the Infill rate at level – 3, Build speed at level – 3 and the build temperature at level – 3. Table 6.6 shows Optimum setting parameters for Tensile strength (UTS).

Table 6.6 Optimum response tables for Tensile strength (UTS)

| **Factors** | **Code** | **Level** | **Optimize value** | |
|---|---|---|---|---|
| **Layer height** | A | 1 | 0.180 mm | **Optimum Value**<br>**UTS =39.094 MPa**<br>**At maximum value of S/N ratio = 31.8422** |
| **Infill** | B | 3 | 45 % | |
| **Build speed** | C | 3 | 180 mm/min | |
| **Build temperature** | D | 3 | 240 $^{o}$c | |

## 6.8 Validation of optimum setting

Experiments were conducted to ensure performance on optimum condition and the result was tabulate in Table 6.7. From the results, it is observe that optimized condition gives good Tensile strength (UTS). The initial reading of Tensile strength was UTS = 39.094 MPa. After setting the parameters to the optimized values, the response characteristic has been changed to UTS = 39.783 MPa.

Table 6.7 Results of the confirmation experiments for optimized condition of mean UTS

| Optimal level | Response obtained | | |
|---|---|---|---|
| | **Initial reading** (predicted result) | **After reading** (Exp. result) | **Error % = 1.732 %** |
| **Mean Tensile strength (UTS)** | 39.094 MPa | 39.783 MPa | $=\frac{(\text{Exp.Result} - \text{predicted result}) * 100}{\text{Experimental result}}$ |

## 6.9 Multiple response optimization

Multiple Optimization of Dimensional accuracy, Surface roughness and Tensile strength done using Taguchi method. Based on Taguchi analysis method, the optimal process parameters for Dimensional accuracy, Surface roughness and Tensile strength are at layer height 0.3422 mm, the Infill rate at 15 % , Build speed at 180 mm/min and the build temperature at 235 ºC. Table 6.8 shows Optimum setting parameters for Dimensional accuracy, Surface roughness and Tensile strength.

Table 6.8 Optimum response tables for Dimensional accuracy, Surface roughness and Tensile strength

| Factors | Code | Optimized values | Optimum Value |
|---|---|---|---|
| **Layer height** | A | 0.3422 mm | % ΔW = 0.01782 at S/N ratio 36.72 |
| **Infill** | B | 15 % | % ΔT = 0.00561 at S/N ratio 45.02 |
| **Build speed** | C | 180 mm/min | % ΔL = 0.005930 at S/N ratio 0.00630 |
| **Build temperature** | D | 235 ºc | Mean Ra = 14.47 µm at S/N ratio -22.56<br>UTS = 32.11 MPa at S/N ratio 30.00 |

# Chapter 7

# CONCLUSION AND SCOPE OF FUTURE WORK

## 7.1 Conclusion

This research presents the Taguchi methods for optimization of Dimensional accuracy (ΔW, ΔT, ΔL), Surface roughness (Ra) and Tensile strength (UTS) on parts produced using Flash forge FDM machine. Taguchi design of experiments L9 orthogonal array were used for experimentation. The impact of process parameters like; layer height, infill, build speed, and build temperature on response output were analyzed using Taguchi analysis, main effect plots, Interaction plots, 3D Surface plots and Contour plots with the help of Minitab V18.1 software. Optimum setting was determined using S/N ratio

### 7.1.1 Dimensional Accuracy (ΔW, ΔT, ΔL)

From the result obtained, the following can be concluded for Dimensional Accuracy (ΔW, ΔT, ΔL):

- Dimensional accuracy (Mean and S/N ratio of relative change in width (ΔW)), is most significantly affected by layer height followed by build temperature, build speed and infill density has insignificant effect.
- Mean and S/N ratio of ΔT infill has most significant factors follow by build temperature, and layer height and build speed.
- Mean and S/N ratio of ΔL layer height has most significant factor affecting change length and build temperature has insignificant effect. Infill rate and build speed have equal impact on percentage change length (ΔL).
- Based on the S/N analysis, the optimal setting of process parameters for dimensional accuracy (ΔW, ΔT, and ΔL) are the layer height at level – 2, the Infill rate at level – 1, Build speed at level – 1 and the build temperature at level – 1.
- The optimum value for dimensional accuracy (ΔW, ΔT and ΔL) through Taguchi method is ΔW = 0.0048 at maximum value of S/N ratio = 46.3752, ΔT = 0.0044 at maximum value of S/N ratio = 47.1309, and % ΔL = 0.0056 at maximum value of S/N ratio = 45.0362.

### 7.1.2 Surface roughness (Ra)

From the result obtained, the following can be concluded for surface roughness (Ra):

- Surface roughness (Ra) has most significantly affected by layer height and Build temperature has insignificant effect.
- Minimum surface roughness can be obtained at middle value of layer height, low infill, high build speed and at middle of build temperature.
- Based on the S/N analysis, the optimal process parameters for surface roughness (Ra) are the layer height at level – 2, the Infill rate at level – 1, Build speed at level – 1 and the build temperature at level – 1.
- The optimum surface roughness value through Taguchi method is Ra = 7.779 µm at maximum value of S/N ratio - 17.8185.

### 7.1.3 Tensile strength (UTS)

From the result obtained, the following conclusion has drawn for Tensile strength (UTS):

- Tensile strength (UTS) has most significantly affected by Build speed followed by infill, build temperature and Layer height has insignificant effect.
- Result of Taguchi optimization indicates that the optimal FDM parameters for Tensile strength (UTS) are the layer height at level – 1, the Infill rate at level – 3, Build speed at level – 3 and the build temperature at level – 3.
- The optimum Tensile strength (UTS) value through Taguchi method is UTS =39.094 MPa at maximum value of S/N ratio = 31.8422.

## 7.2 Contribution of the research work

Many researchers tend to evaluate process parameters in FDM to satisfy the functional requirements of the manufacturing process such as accuracy, build time, strength and efficiency of the process. From previous investigations, it has been agreed that the evaluation of parameters can lead to the improvement of the process of FDM. Thus, the identification of the significant factors in the FDM build process can lead to the development of a more precise and repeatable process. Consequently, the quality characteristics of building parts can be more accurate and predicted, since prototypes are used as a master pattern in secondary manufacturing processes or as a final part. This research attempts to identify key parameter settings that influence output response according to their desired build preferences. Hence, the FDM process can be made more efficient, whilst developing a manufacturing process plan that offers comprehensive data to the FDM users to predicted output response characteristics. Future experiments and evaluation of parameters will lead to the creation of knowledge system based on data in order to provide recommendations for optimal process variable settings and according to the design preferences, such as reducing building time and cost, increasing tensile strength or minimizing surface roughness of processed FDM parts.

### 7.3 Recommendations for future works

The present work leaves a wide scope for future investigators to explore many aspects of FDM and other RP processes on similar lines. Some recommendations for future research include:

- Different optimization technique can be repeat the same experiment with the same level and parameters.
- The effects of environmental variables like temperature and humidity on the part quality need to be explored.
- Applicability of FDM from small size batch production to medium or large batch sizes can be extended by increasing the build space and providing multiple nozzles for material deposition.
- Option of depositing multiple materials in a single setting and necessary changes in hardware need to be explored.
- Possibility of using different materials or modifications in the present material composition can be explored.
- Study the effect of other parameters such as; infill angle, number of contours, contour width, raster width, air gap, raster orientation, raster angle, layer thickness, build style and etc.
- Explore impact of FDM process parameters on other quality responses, such as other mechanical properties (flexural strength, modulus of elasticity, elongation at break, flexural modulus), build time, part shrinkage and etc.

## Reference


[1] R. Nagpal, R. Gupta, and V. Gupta, "A review on trends and development of rapid prototyping processes in industry," *A Rev. trends Dev. rapid Prototyp. Process. Ind.*, vol. 2, no. 4, pp. 224–228, 2017.

[2] P. Dudek, "FDM 3D printing technology in manufacturing composite elements," *Arch. Metall. Mater.*, vol. 58, no. 4, pp. 1415–1418, 2013.

[3] C. W. Gomes, "Rapid Prototyping," *Assem. Autom.*, vol. 13, no. 1, p. 3, 2000.

[4] R. Narang and D. Chhabra, "Analysis of Process Parameters of Fused Deposition Modeling ( FDM ) Technique," *Int. J. Futur. Revolut. Comput. Sci. Commun. Eng.*, vol. 3, no. October 2017, pp. 41–48, 2017.

[5] B. Huang and S. Singamneni, "Alternate slicing and deposition strategies for fused deposition modelling of light curved parts," *J. Achiev. Mater. Manuf. Eng.*, vol. 55, no. 2, p. 511, 2012.

[6] A. R. A. & M. A. E. Azhar Equbal, Anoop Kumar Sood, "Optimization of Process Parameters of FDM Part for Minimiizing its Dimensional Inaccuracy," *Int. J. Mech. Prod. Eng. Res. Dev.* , vol. 7, no. 2, pp. 57–66, 2017.

[7] S. O. Akande, "Dimensional Accuracy and Surface Finish Optimization of Fused Deposition Modelling Parts using Desirability Function Analysis," *Int. J. Eng. Res. Technol.*, vol. 4, no. 04, pp. 196–202, 2015.

[8] K. Leivisk, "Introduction to experiment design," 2013.

[9] V. Sharma and S. Singh, "Rapid Prototyping : Process advantage , comparison and application," *Int. J. Comput. Intell. Res.*, vol. 12, no. 1, pp. 55–61, 2016.

[10] "Rapid prototyping - Wikipedia," 2018. .

[11] O. Y. Venkatasubbareddy, P. Siddikali, and S. M. Saleem, "Improving the Dimensional Accuracy And Surface Roughness of Fdm Parts Using Optimization Techniques," *Improv. Dimens. Accuracy Surf. Rough. Fdm Parts Using Optim. Tech. O.Y.Venkatasubbareddy1,*

pp. 18–22, 2010.

[12] S. K. Gurunathan and K. Krishnan, "Surface roughness investigation and prediction models for poly-jet 3D printed Surface roughness investi- gation and prediction models for poly-jet 3D printed parts This conference article should be cited as :," *Surf. Rough. Investig. pridiction Model. poly -jet 3D Print. parts*, no. February 2016, pp. 1–8, 2013.

[13] D. M. Calandra, D. Di Mauro, F. Cutugno, and S. Di Martino, "Navigating wall-sized displays with the gaze: A proposal for cultural heritage," *CEUR Workshop Proc.*, vol. 1621, no. May 2014, pp. 36–43, 2016.

[14] I. T. E. P. A. Per, "Introduction to Desktop Stereolithography," no. March, 2015.

[15] S. I. Ruiz, M. A. Frias, and A. G. Rider, Ricardo Martínez; Guillen, Amaury Pozos; Rangel, "Fundamentals of Stereolithography , an Useful Tool for Diagnosis in Dentistry," *Odovtos Int. J. Dent. Sci.*, vol. 17, no. 1, pp. 15–21, 2015.

[16] M. Saffarzadeh, G. James Gillispie, and P. Brown, "Selective Laser Sintering (Sls) Rapid Protytping Technology: a Review of Medical Applications," no. April, 2016.

[17] W. R. Ng, "Tutorial : Rapid Prototyping Technologies," *Opti 521*, pp. 1–10, 2010.

[18] X. Tian, G. Peng, M. Yan, S. He, and R. Yao, "Process prediction of selective laser sintering based on heat transfer analysis for polyamide composite powders," *Int. J. Heat Mass Transf.*, vol. 120, no. nternational Journal of Heat and Mass Transfer 120 (2018) 379–386 Contents, pp. 379–386, 2018.

[19] B. Duan and M. Wang, "Selective laser sintering and its application in biomedical engineering," *MRS Bull.*, vol. 36, no. 12, pp. 998–1005, 2011.

[20] M. Feygin, *Laminated object manufacturing*, vol. 3.10, no. D. 1989, pp. 1–2.

[21] Azo Materials, "Rapid Prototyping - Laminated Object Modelling and Computer Aided Manufacturing of Laminated Engineering Materials," *Azo Materials*. p. http://www.azom.com/article.aspx?ArticleID=1650, 2013.

[22] A. Levchenko, "Additive manufacturing as a mean of rapid prototyping : from words to

the actual model," 2015.

[23] "FDM technology: The advantages of FDM printing | dddrop." [Online]. Available: https://www.dddrop.com/fdm-technology/.

[24] S. Kumar, V. Kannan, and G. Sankaranarayanan, "Parameter Optimization of ABS-M30i Parts Produced by Fused Deposition Modeling for Minimum Surface Roughness," *Int. J. Curr. Eng. Technol.*, no. 3, pp. 93–97, 2014.

[25] O. Lužanin, D. Movrin, and M. Plan, "Effect of Layer Thickness , Deposition Angle , and Infill on Maximum Flexural Force in Fdm-Built Specimens," *J. Technol. Plast.*, vol. 39, no. 1, pp. 49–58, 2014.

[27] W. Wu, W. Ye, Z. Wu, P. Geng, Y. Wang, and J. Zhao, "Influence of layer thickness, raster angle, deformation temperature and recovery temperature on the shape-memory effect of 3D-printed polylactic acid samples," *Materials (Basel).*, vol. 10, no. 8, pp. 1–16, 2017.

[28] C. Dudescu and L. Racz, "Effects of Raster Orientation, Infill Rate and Infill Pattern on the Mechanical Properties of 3D Printed Materials," *ACTA Univ. Cibiniensis*, vol. 69, no. 1, pp. 1–30, 2017.

[29] B. Jawalkar, A. Shirke, and T. Satpute, "Tensile test and fea correlation of abs plastic," no. 6, pp. 33–37, 2015.

[30] J. Cantrell *et al.*, "Experimental Characterization of the Mechanical Properties of 3D Printed ABS and Polycarbonate Parts," pp. 89–105, 2017.

[31] N. Saleh, S. Mansour, and R. Hague, "Investigation into the mechanical properties of rapid manufacturing materials," *Solid Free. Fabr. Symp. Proc.*, pp. 287–296, 2002.

[32] K. Raney, E. Lani, and D. K. Kalla, "Experimental characterization of the tensile strength of ABS parts manufactured by fused deposition modeling process," *Mater. Today Proc.*, vol. 4, no. 8, pp. 7956–7961, 2017.

[33] P. B. Patel, J. D. Patel, and K. D. Maniya, "Evaluation of FDM Process Parameter for

PLA Material by Using MOORA-TOPSIS Method," vol. 3, no. 1, pp. 84–93, 2015.

[34] G. Arumaikkannu, N. A. Kumar, and R. Saravanan, "Study on the influence of rapid prototyping parameters on product quality in 3d printing," *19th Annu. Int. Solid Free. Fabr. Symp. SFF 2008*, pp. 495–506, 2008.

[35] X. Zhang *et al.*, "Response surface methodology used for statistical optimization of jieanpeptide production by Bacillus subtilis," *Electron. J. Biotechnol.*, vol. 13, no. 4, 2010.

[36] S. Adamczak, P. Zmarzly, T. Kozior, and D. Gogolewski, "Analysis of the dimensional accuracy of casting models manufactured by fused deposition modeling technology," *Eng. Mech. 2017*, no. May, pp. 66–69, 2017.

[37] T. N. A. Tuan Rahim, H. M. Akil, A. M. Abdullah, D. Mohamad, and Z. A. Rajion, "Optimization of the 3D printing parameters on dimensional accuracy and surface finishing for new polyamide 6 and its composite used in fused deposition modeling (FDM) process," *J. Mech. Eng.*, vol. SI 4, no. 2, pp. 75–90, 2017.

[38] M. N. Sudin, S. A. Shamsudin, and M. A. Abdullah, "Effect of part features on dimensional accuracy of fdm model," *ARPN J. Eng. Appl. Sci.*, vol. 11, no. 13, pp. 8067–8072, 2016.

[39] N. A. Sukindar *et al.*, "Optimization of the Parameters for Surface Quality of the Open-source 3D Printing," vol. 3, no. 1, pp. 33–43, 2017.

[40] A. Kohad, R. Dalu, and P. G. Student, "Optimization of Process Parameters in Fused Deposition Modeling: A Review," *Int. J. Innov. Res. Sci. Eng. Technol. An ISO*, vol. 3297, no. 1, pp. 505–511, 2007.

[41] F. Ali and J. Maharaj, "Influence of some process parameters on build time, material consumption and surface roughness of FDM processed parts: Inferences based on the Taguchi design of experiments.," *Proc. 2014 IAJC/ISAM Jt. Int. Conf.*, 2014.

[42] PandeyM. and Pulak, "Rapid prototyping technologies, applications and part deposition planning," *Retrieved Oct.*, no. June, p. 15, 2010.

[43] J. Jiang, X. Xu, and J. Stringer, "Support Structures for Additive Manufacturing: A Review," *J. Manuf. Mater. Process.*, vol. 2, no. 4, p. 64, 2018.

[44] P. Vasconcelos, F. Lino, R. Neto, and M. Vasconcelos, "Design and Rapid Prototyping Evolution," *Adv. Solut. Dev.*, pp. 1–4, 2002.

[45] N. M. Anoosha, B. Sachin, B. R. Hemanth, P. K. K. P, and N. Yathisha, *Tensile test & FEM Analysis of ABS material using FDM Technique*. 2018, pp. 6658–6663.

[46] M. Kobayashi and T. Nakajima, "Medical application of rapid prototyping," *Seimitsu Kogaku Kaishi/Journal Japan Soc. Precis. Eng.*, vol. 70, no. 2, pp. 179–182, 2004.

[47] T. Kucklick, "Medical Applications of Rapid Technologies," *Med. Device R&D Handbook, Second Ed.*, no. January 2007, pp. 167–182, 2012.

[48] L. C. Hieu *et al.*, "Medical rapid prototyping applications and methods," *Assem. Autom.*, vol. 25, no. 4, pp. 284–292, 2005.

[49] S. Singare *et al.*, "Rapid prototyping assisted surgery planning and custom implant design," *Rapid Prototyp. J.*, vol. 15, no. 1, pp. 19–23, 2009.

[50] H. Kheirollahi and F. Abbaszadeh, "Application of rapid prototyping technology in dentistry," *Int. J. Rapid Manuf.*, vol. 2, no. 1/2, p. 104, 2011.

[51] L. Sabadin Bertol, F. P. da Silva, and W. Kindlein Junior, "Design and health care: A study of virtual design and direct metal laser sintering of titanium alloy for the production of customized facial implants," *Australas. Med. J.*, vol. 2, no. 11, pp. 136–141, 2009.

[52] C. Surgical, S. Infections, and P. Participants, "Joint Commission Center for Transforming Health Care Reducing Colorectal Surgical Site Infections Colorectal Surgical Site Infection Project Outline," vol. 95, no. 11, pp. 4–5, 2014.

[53] H. I. Medellín-Castillo and J. E. Pedraza Torres, "Rapid Prototyping and Manufacturing: A Review of Current Technologies," *Vol. 4 Des. Manuf.*, no. January 2009, pp. 609–621, 2009.

[54] I. Campbell, D. Bourell, and I. Gibson, "Additive manufacturing: rapid prototyping comes

of age," *Rapid Prototyp. J.*, vol. 18, no. 4, pp. 255–258, 2012.

[55] R. J. Bateman and K. Cheng, "Rapid Manufacturing as a tool for agile manufacturing : application and implementation perspectives," no. May 2014, 2006.

[56] R. Udroiu and N. V Ivan, "Rapid Prototyping and Rapid Manufacturing Applications At," vol. 3, no. 52, 2010.

[57] S. Wannarumon and E. L. J. Bohez, "Rapid Prototyping and Tooling Technology in Jewelry CAD," *Comput. Aided. Des. Appl.*, vol. 1, no. 1–4, pp. 569–575, 2004.

[58] N. P. Karapatis, J. P. S. Van Griethuysen, and R. Glardon, "Direct rapid tooling: A review of current research," *Rapid Prototyp. J.*, vol. 4, no. 2, pp. 77–89, 1998.

[59] D. Ph and M. Engineering, "Rapid Prototyping/Rapid Tooling–A Over View And Its Applications In Orthopaedics," *J. Adv.*, pp. 1–14, 2011.

[60] N. Z. Ć. Ć and S. Lemeš, "Applications of rapid tooling techniques for injection moulding," pp. 21–24.

[61] Y. Ding, H. Lan, J. Hong, and D. Wu, "An integrated manufacturing system for rapid tooling based on rapid prototyping," *Robot. Comput. Integr. Manuf.*, vol. 20, no. 4, pp. 281–288, 2004.

[62] F. Joubert, "Rapid Tooling and the LOMOLD Process," 2005.

[63] N. K. Dixit, R. Srivastava, and R. Narain, "Comparison of Two Different Rapid Prototyping System Based on Dimensional Performance Using Grey Relational Grade Method," *Procedia Technol.*, vol. 25, no. Raerest, pp. 908–915, 2016.

[64] R. Agarwal and R. Singh, "Experimental analysis of surface roughness and dimensional accuracy of abs - ssd 0150 fdm components," vol. 5, no. 04, pp. 73–86, 2017.

[65] T. Dalgleish *et al.*, "[ No Title ]," *J. Exp. Psychol. Gen.*, vol. 136, no. 1, pp. 23–42, 2007.

[66] P. Cătălin IANCU, E. Daniela IANCU, and D. Alin STĂNCIOIU, "From Cad Model to 3D Print Via STL Format," *Acad. Brâncuşi Târgu Jiu*, vol. 1, no. 1, pp. 1844–640, 2010.

[67] A. K. Sood, R. K. Ohdar, and S. S. Mahapatra, "Grey Taguchi Method for Improving Dimensional Accuracy of FDM Process," *Mater. Des.*, vol. 30, no. 10, pp. 4243–4252, 2009.

[67] F. Górski, W. Kuczko, and R. Wichniarek, "Influence of Process Parameters on Dimensional Accuracy of Parts Manufactured Using Fused Deposition Modelling Technology," *Adv. Sci. Technol. – Res. J.*, vol. 7, no. 19, pp. 27–35, 2013.

[68] O. A. Mohamed, S. H. Masood, and J. L. Bhowmik, "Optimization of fused deposition modeling process parameters for dimensional accuracy using I-optimality criterion," *Meas. J. Int. Meas. Confed.*, vol. 81, pp. 174–196, 2016.

[69] N. Tran, V. Nguyen, A. Ngo, and V. Nguyen, "Study on the Effect of Fused Deposition Modeling ( FDM ) Process Parameters on the Printed Part Quality," *Ngoc-Hien Tran. Int. J. Eng. Res. Appl.*, vol. 7, no. 12, pp. 71–77, 2017.

[70] Y. S. Dambatta and A. A.D.Sarhan, "surface roughness Analysis,Modelling and prediction in fused depostion modeling additive manifacturing technology," *World Acad. Sci. Eng. Technol. Int. J. Ind. Manuf. Eng.*, vol. 10, no. 8, pp. 1582–1589, 2016.

[71] G. S. Bual, "Methods to Improve Surface Finish of Parts Produced by Fused Deposition Modeling," *Manuf. Sci. Technol.*, vol. 2, no. 3, pp. 51–55, 2014.

[72] O. A. Mohamed, S. H. Masood, and J. L. Bhowmik, "Mathematical modeling and FDM process parameters optimization using response surface methodology based on Q-optimal design," *Appl. Math. Model.*, vol. 40, no. 23–24, pp. 10052–10073, 2016.

[73] D. Cristian, M. Engineering, M. Engineering, R. L. Ph, M. Engineering, and M. Engineering, "Effects of raster orientation,infill rate and infill pattern on mechanichal properties of 3D printed materials," Romania, 2017.

[74] F. Rayegani and G. C. Onwubolu, "Fused deposition modelling ( FDM ) process parameter prediction and optimization using group method for data handling ( GMDH ) and differential evolution ( DE )," *Int J AdvManuf Technol*, vol. 2, pp. 1–11, 2014.

[75] J. M. Chacón, M. A. Caminero, E. García-Plaza, and P. J. Núñez, "Additive

manufacturing of PLA structures using fused deposition modelling: Effect of process parameters on mechanical properties and their optimal selection," *Mater. Des.*, vol. 124, pp. 143–157, 2017.

# Appendices

## Appendix A: Dimension of printed parts

Figure A.1 Figure of printed part with dimension

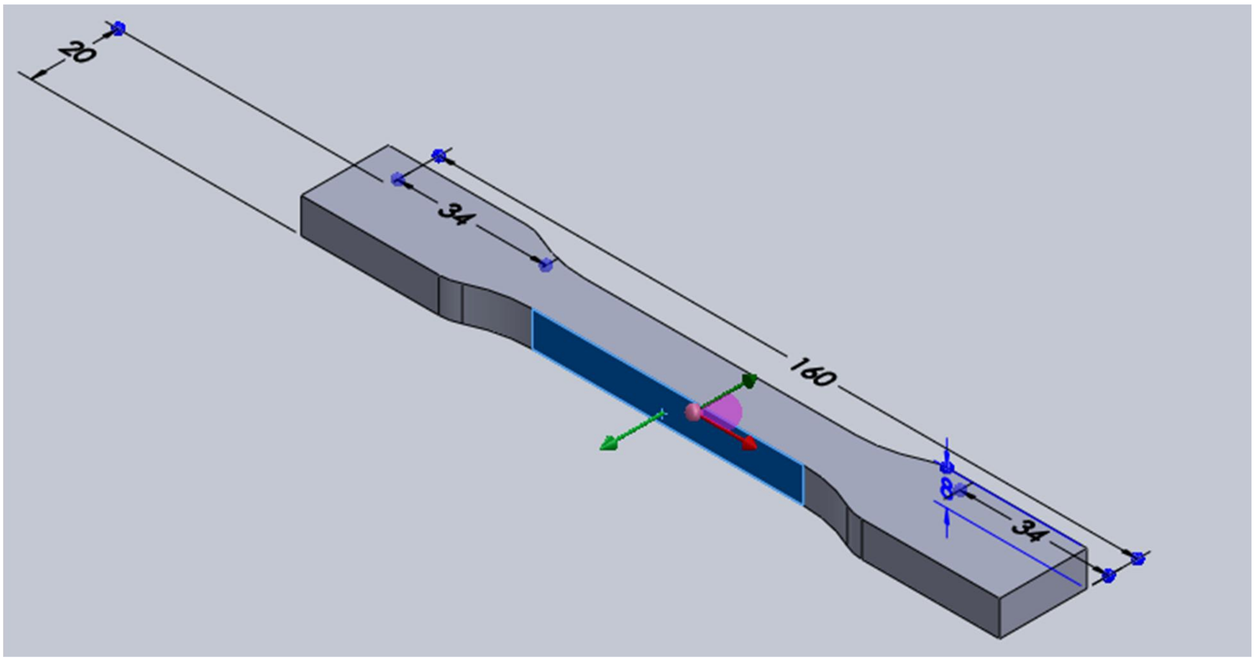


Table A.2 Dimension OF printed part

| Dimension abbreviation list | Measurement (mm) |
|---|---|
| W – Width of narrow section | 12 |
| L – Length of narrow section | 80 |
| WO – Width of overall | 20 |
| LO – Length overall | 160 |
| D – Distance between grips | 100 |

## Appendix B: Result of experimental data for estimated material and manufacturing time

Table B.1 Result estimated material and manufacturing time

| Exp. trial | Input parameters | | | | Response | |
|---|---|---|---|---|---|---|
| | A | B | C | D | Estimated material | Manufacturing Time |
| 1 | 0.180 | 15 | 60 | 220 | 4.0209 m | 49 minutes |
| 2 | 0.180 | 30 | 120 | 230 | 3.6093 m | 62 minutes |
| 3 | 0.180 | 45 | 180 | 240 | 4.6285 m | 88 minutes |
| 4 | 0.290 | 15 | 60 | 220 | 5.6742 m | 35 minutes |
| 5 | 0.290 | 30 | 120 | 230 | 4.0498 m | 42 minutes |

| | | | | | | |
|---|---|---|---|---|---|---|
| 6 | 0.290 | 45 | 180 | 240 | 5.990 m | 52 minutes |
| 7 | 0.40 | 15 | 60 | 220 | 4.640 m | 30 minutes |
| 8 | 0.40 | 30 | 120 | 230 | 5.490 m | 32 minutes |
| 9 | 0.40 | 45 | 180 | 240 | 6.330 m | 39 minutes |

## Appendix C: Result of experimental data for dimensional accuracy

Table C.1 Result of experimental data of ΔW

| EXP. trials | Input parameters | | | | Relative change in dimension of Width | | | | | | |
|---|---|---|---|---|---|---|---|---|---|---|---|
| | **A** | **B** | **C** | **D** | **Trial 1** | **Trial 2** | **Trial 3** | **Trial 4** | **Trial 5** | **Mean ΔW** | **SNRA1** |
| 1 | 0.180 | 15 | 60 | 220 | 0.015 | 0.0028 | 0.023 | 0.0833 | 0.0088 | 0.0266 | 31.5024 |
| 2 | 0.180 | 30 | 120 | 230 | 0.013 | 0.0186 | 0.0217 | 0.0167 | 0.008 | 0.0156 | 36.1375 |
| 3 | 0.180 | 45 | 180 | 240 | 0.0088 | 0.0283 | 0.0133 | 0.0313 | 0.0063 | 0.0176 | 35.0897 |
| 4 | 0.290 | 15 | 60 | 220 | 0.0013 | 0.0062 | 0.0022 | 0.0083 | 0.0063 | 0.0048 | 46.3752 |
| 5 | 0.290 | 30 | 120 | 230 | 0.0063 | 0.0117 | 0.0217 | 0.025 | 0.0113 | 0.0152 | 36.3631 |
| 6 | 0.290 | 45 | 180 | 240 | 0.0088 | 0.0145 | 0.0167 | 0.0104 | 0.0003 | 0.0102 | 39.8280 |
| 7 | 0.40 | 15 | 60 | 220 | 0.008 | 0.02 | 0.03 | 0.0228 | 0.015 | 0.0192 | 34.3340 |
| 8 | 0.40 | 30 | 120 | 230 | 0.01 | 0.0187 | 0.03 | 0.0271 | 0.015 | 0.0202 | 33.8930 |
| 9 | 0.40 | 45 | 180 | 240 | 0.013 | 0.0117 | 0.0313 | 0.0283 | 0.015 | 0.0199 | 34.0229 |

Table C.2 Result of experimental data of ΔT

| **EXP. trials** | **Input parameters** | | | | **Relative change in dimension of thickness** | | | | | | |
|---|---|---|---|---|---|---|---|---|---|---|---|
| | **A** | **B** | **C** | **D** | **Trial 1** | **Trial 2** | **Trial 3** | **Trial 4** | **Trial 5** | **Mean ΔT** | **SNRA1** |
| 1 | 0.180 | 15 | 60 | 220 | 0.0032 | 0.0156 | 0.0032 | 0.0125 | 0.0032 | 0.0075 | 42.4988 |
| 2 | 0.180 | 30 | 120 | 230 | 0.0062 | 0.0093 | 0.0032 | 0.0093 | 0.0156 | 0.0087 | 41.2096 |
| 3 | 0.180 | 45 | 180 | 240 | 0.0032 | 0.0125 | 0.0062 | 0.0156 | 0.0156 | 0.0106 | 39.4939 |
| 4 | 0.290 | 15 | 60 | 220 | 0.0032 | 0.0032 | 0.0062 | 0.0032 | 0.0062 | 0.0044 | 47.1309 |
| 5 | 0.290 | 30 | 120 | 230 | 0.0062 | 0.0032 | 0.0156 | 0.0175 | 0.0125 | 0.011 | 39.1721 |

| | | | | | | | | | | | |
|---|---|---|---|---|---|---|---|---|---|---|---|
| 6 | 0.290 | 45 | 180 | 240 | 0.0125 | 0.0156 | 0.0175 | 0.0218 | 0.0032 | 0.0141 | 37.0156 |
| 7 | 0.40 | 15 | 60 | 220 | 0.0032 | 0.0062 | 0.0032 | 0.0093 | 0.0062 | 0.0056 | 45.0362 |
| 8 | 0.40 | 30 | 120 | 230 | 0.0125 | 0.0062 | 0.0156 | 0.0032 | 0.0125 | 0.01 | 40.0000 |
| 9 | 0.40 | 45 | 180 | 240 | 0.0093 | 0.0062 | 0.0062 | 0.0156 | 0.0175 | 0.0109 | 39.2515 |

Table C.3 Result of experimental data of ΔL

| EXP. trials | Input parameters | | | | Relative change in dimension of length | | | | | | |
|---|---|---|---|---|---|---|---|---|---|---|---|
| | A | B | C | D | Trial 1 | Trial 2 | Trial 3 | Trial 4 | Trial 5 | Mean ΔL | SNRA1 |
| 1 | 0.180 | 15 | 60 | 220 | 0.00625 | 0.00619 | 0.00612 | 0.006 | 0.00587 | 0.0061 | 44.2934 |
| 2 | 0.180 | 30 | 120 | 230 | 0.0061 | 0.00607 | 0.00625 | 0.00612 | 0.00615 | 0.0061 | 44.2934 |
| 3 | 0.180 | 45 | 180 | 240 | 0.006 | 0.00597 | 0.00595 | 0.00525 | 0.0052 | 0.0057 | 44.8825 |
| 4 | 0.290 | 15 | 60 | 220 | 0.00615 | 0.00607 | 0.0051 | 0.00607 | 0.0042 | 0.0056 | 45.0362 |
| 5 | 0.290 | 30 | 120 | 230 | 0.0061 | 0.00607 | 0.00602 | 0.00607 | 0.00615 | 0.0061 | 44.2934 |
| 6 | 0.290 | 45 | 180 | 240 | 0.00602 | 0.0061 | 0.00615 | 0.00595 | 0.00602 | 0.0060 | 44.4370 |
| 7 | 0.40 | 15 | 60 | 220 | 0.00607 | 0.0061 | 0.00587 | 0.00581 | 0.00595 | 0.0059 | 44.5830 |
| 8 | 0.40 | 30 | 120 | 230 | 0.006 | 0.00602 | 0.00606 | 0.00605 | 0.00595 | 0.0060 | 44.4370 |
| 9 | 0.40 | 45 | 180 | 240 | 0.00602 | 0.00615 | 0.00619 | 0.00609 | 0.00597 | 0.0061 | 44.2934 |

## Appendix D: Result of experimental data for surface roughness

Table D.1 Result of experimental data of surface roughness

| EXP. trials | Input parameters | | | | Response | | | | | | |
|---|---|---|---|---|---|---|---|---|---|---|---|
| | A | B | C | D | Trial 1 | Trial 2 | Trial 3 | Trial 4 | Trial 5 | Mean Ra µm | SNRA1 |
| 1 | 0.180 | 15 | 60 | 220 | 19.20 | 17.34 | 17.45 | 15.38 | 14.94 | 16.862 | -24.5382 |
| 2 | 0.180 | 30 | 120 | 230 | 12.65 | 20.83 | 24.43 | 18.22 | 13.41 | 17.908 | -25.0609 |
| 3 | 0.180 | 45 | 180 | 240 | 12.11 | 14.94 | 8.073 | 11.07 | 12.38 | 11.703 | -21.3659 |
| 4 | 0.290 | 15 | 60 | 220 | 6.436 | 7.528 | 8.128 | 8.401 | 8.401 | 7.779 | -17.8185 |
| 5 | 0.290 | 30 | 120 | 230 | 7.637 | 10.14 | 9.219 | 10.25 | 8.128 | 9.074 | -19.1560 |

| | | | | | | | | | | | |
|---|---|---|---|---|---|---|---|---|---|---|---|
| 6 | 0.290 | 45 | 180 | 240 | 8.401 | 9.164 | 9.328 | 7.528 | 87.091 | 8.302 | -18.3837 |
| 7 | 0.40 | 15 | 60 | 220 | 15.60 | 15.05 | 11.23 | 9.982 | 12.27 | 12.826 | -22.1618 |
| 8 | 0.40 | 30 | 120 | 230 | 29.45 | 24.98 | 19.31 | 17.78 | 22.47 | 22.798 | -27.1579 |
| 9 | 0.40 | 45 | 180 | 240 | 23.23 | 18.98 | 24.98 | 17.78 | 22.25 | 21.44 | -26.6245 |